The antibacterial T6SS of *Agrobacterium tumefacien* promotes disease occurrence and influences crown gall microbiota composition

Si-Chong Wang[1,2], Ai-Ping Chen[1], Shu-Jen Chou[1], Chih-Horng Kuo[1*], Erh-Min Lai[1*]

[1] Institute of Plant and Microbial Biology, Academia Sinica, Taipei, Taiwan,
[2] Department of Life Science, National Central University, Taoyuan, Taiwan

Running title: T6SS on tumorigenesis and gallobiome

*Corresponding authors
Erh-Min Lai: emlai@gate.sinica.edu.tw
Chih-Horng Kuo: chkuo@gate.sinica.edu.tw
Institute of Plant and Microbial Biology, Academia Sinica
128, Sec. 2, Academia Road, Nankang, Taipei, Taiwan 11529

ORCID
CHK https://orcid.org/0000-0002-2857-0529
EML https://orcid.org/0000-0003-3630-8683
SCW https://orcid.org/0000-0002-6192-8844

Keywords: *Agrobacterium tumefaciens*, crown gall, type VI secretion system, microbiota, 16S rRNA gene amplicon sequencing

ABSTRACT

The type VI secretion system (T6SS) is deployed by many proteobacteria to secrete effector proteins into bacterial competitors for competition or eukaryotic cells for pathogenesis. *Agrobacterium tumefacien*, a soil-borne phytopathogen causing crown gall disease on various plant species, deploys its T6SS to attack closely- and distantly-related bacterial species *in vitro* and *in planta*. Current evidence suggests that the *A. tumefaciens* T6SS is not essential for pathogenesis under direct inoculation but it remains unknown whether T6SS influences natural disease incidence and microbial community of crown galls. To address these two key questions, we established a soil inoculation method on wounded tomato seedlings that mimics natural infections and performed 16S rRNA gene amplicon sequencing. By comparing the *A. tumefaciens* C58 wild-type strain with two T6SS mutants, we demonstrate that the T6SS influences disease occurrence and microbiota composition within crown galls. Based on multiple inoculation trials across seasons, all three strains could induce tumors but the mutants had significantly lower disease incidences. The season of inoculation played a more important role than the T6SS in shaping the gall microbiota (i.e., gallobiome). The influence of T6SS was evident in summer, in which two bacterial families (Sphingomonadaceae and Burkhoderiaceae) were enriched in the gallobiome induced by the T6SS mutants. Further *in-vitro* competition and colonization assay demonstrated the T6SS-mediated antagonism to a tomato isolate *Sphingomonas* sp. R1. In conclusion, this study informs that the *A. tumefaciens* T6SS may promote tumorigenesis in natural infection process and provide competitive advantages in gall-associated microbiota.

IMPORTANCE

T6SS is widespread in the agrobacterial genome and used by *Agrobacterium tumefaciens* for interbacterial competition. *A. tumefaciens* is a soil inhabitant and opportunistic bacterial pathogen causing crown gall disease in wide range of plants. Current evidence indicates that T6SS is not required for gall formation when the agrobacteria are inoculated directly on plant wounding sites. However, in terms of disease ecology, agrobacteria may need to compete with other bacteria in bulk soil to gain access to plant wounds and influence microbial community inside crown galls. To date, the role of T6SS in agrobacterial pathogenesis and gallobiome under a more natural setting remains unknown. In this study, we successfully developed a soil inoculation method coupled with a Blocker-mediated Bacterial 16S rRNA gene amplicon Enrichment Sequencing (BBRES) to address these two important questions.

We provided evidence that T6SS promotes disease occurrence and influences crown gall microbiota composition by interbacterial competition.

INTRODUCTION

Many proteobacteria, including pathogens and commensals, deploy the type VI secretion system (T6SS) for antagonism or pathogenesis (1, 2) . It is a protein translocation apparatus used to inject effectors into target cells, mainly in a contact-dependent manner. Based on the destination and biological function of known effectors (3), T6SS mainly functions as an antibacterial weapon used by bacteria to inhibit or kill the competing bacterial species, thus impacting their survival or shaping microbiota in their ecological niche (4).

Previous studies on the microbiome associated with animal guts or plants indicated that the T6SS genes are enriched in these communities, suggesting T6SS may be important for niche competition (5-8). Metagenomic analysis of human gut microbiota revealed a role of T6SS for the domination of the gut symbiont *Bacteroides fragilis* by targeting other members of microbiome *in vitro* and *in vivo* (6, 7). A recent study further showed that a murine pathogen *Citrobacter rodentium* and resident commensal Enterobacteriaceae share the same strategy by using T6SS for niche competition in the murine gastrointestinal tract (9). T6SS is also deployed by plant pathogens to gain competitive growth advantage *in planta* as well as for beneficial bacteria to prevent or reduce disease symptoms caused by competing pathogens (10-12). Comparative metagenomic analysis of microbiota between $T6SS^+$ and $T6SS^-$ bacterial strains were also carry out. The gut microbiota of pests infected by *Pseudomonas protegens,* a plant-beneficial bacterium capable of invading insect pests, showed that T6SS has no significant impact on microbiota diversity at phylum/class level but affects the abundance of Enterobacteriaceae (13). These studies collectively suggest that T6SS is a potent antibacterial weapon used by invading pathogens or resident bacteria to gain competitive advantage in their ecological niche. However, the knowledge into the degree of T6SS in shaping microbiota and the molecular mechanisms of interbacterial competition in complex microbial community are limited.

101 Agrobacteria are a group of bacteria capable of inducing crown gall or hairy root
102 disease on plants by transferring a piece of DNA named T-DNA from bacteria into
103 plants via the type IV secretion system (T4SS) (14). T6SS is highly conserved in the
104 *Agrobacterium tumefaciens* species complex and plays a role in interbacterial
105 competition (15-17). In *A. tumefaciens,* the T6SS is encoded by a gene cluster
106 consisting of an *imp* operon encoding components for T6SS and an *hcp* operon
107 encoding the puncturing device and effectors. Using *A. tumefaciens* reference strain
108 C58, we previously discovered that it uses Tde DNase effectors as the major
109 antibacterial weapon to gain competitive growth advantage to its siblings lacking the
110 cognate immunity protein or other bacterial species by co-infiltration into leaves of
111 *Nicotiana benthamiana* (10). Interestingly, agrobacteria with incompatible effector-
112 immunity (EI) pairs exhibit strong antagonism at the between species level, while
113 only weak or non-detectable effect at the within species level (15). Moreover, higher
114 T6SS-mediated killing outcome was observed when nutrient is scarce, as opposed to
115 nutrient rich condition (18). Thus, genetic and environmental factors beyond EI pairs
116 also contributes to interbacterial competition.
117
118 To date, agrobacterial T6SS has been demonstrated as an antibacterial weapon (15-
119 17). No evidence for its role in promoting virulence when tumor assays were
120 conducted in sterile condition or directly inoculated on the stems of various plant
121 species including tomato plants (19). Considering that agrobacteria may need to
122 compete with other bacteria in bulk soil or rhizosphere to gain access to plant wounds
123 for inciting crown galls, we reasoned that T6SS may influence microbial community
124 and pathogenesis under a more natural setting. To address these questions, we
125 developed a soil inoculation protocol to mimic natural infection on wounded tomato
126 seedlings across seasons for evaluating the impact of the *A. tumefaciens* T6SS on
127 disease occurrence and crown gall microbiota (termed gallobiome). Based on 16S
128 rRNA amplicon sequencing analysis, followed by *in-vitro* competition and
129 colonization assays, the results informed that the T6SS may help *A. tumefaciens* to
130 maintain a stable colonization for competitive advantage on plant surface for effective
131 infection, leading to higher disease incidence.
132
133 **RESULTS**

134

135 **T6SS mutants of *A. tumefaciens* C58 induced lower crown gall disease**
136 **incidences, which was also affected by environmental factors**

137 *Agrobacterium tumefaciens* C58 wild type (WT) and two T6SS mutants with deletion
138 of essential T6SS genes, Δ*tssL* and Δ*tssB* respectively, were used to study the effects
139 of T6SS in tumorigenesis using soil inoculation method. Nine batches of inoculation
140 experiments across different seasons were conducted in this study (Table 1). In total,
141 139 crown galls were collected, including 70 induced by WT, 41 induced by Δ*tssL*,
142 and 28 induced by Δ*tssB*. The results showed that all three strains are capable of
143 inducing tumors, but the disease incidences of Δ*tssL* and Δ*tssB* were significantly
144 lower than WT (Table 1, Fig. 1A). There was no significant weight difference among
145 the crown galls induced by different strains (Fig. 1B). It is notable that the disease
146 incidences of those inoculated in June and July were significantly lower than those in
147 October and November, resulting in an inverse correlation between disease incidence
148 and temperature across seasons for both WT and T6SS mutants throughout the year
149 (Fig. 1C, 1D). These results indicated that both the strains and month of inoculation
150 affected the disease incidence under soil inoculation condition.

151

152 **Round I of 16S rRNA amplicon sequencing: Initial trial**

153 To determine the gallobiome composition, crown galls with similar weights across
154 seasons were selected for 16S rRNA gene amplicon sequencing. For Round I, six
155 crown gall DNA samples, three induced by WT and three by Δ*tssL* were amplified
156 with two commonly used 16S rRNA gene primer sets V3-4 and V5-7 (Table S1). The
157 Illumina sequencing produced 140,830 and 601,299 reads from V3-4 and V5-7 sets,
158 respectively. However, the majority (99.1% in V3-4 and 93.6% for V5-7) of these
159 reads were derived from plant chloroplast and mitochondria. After removing these
160 host contaminations, only 1,230 and 38,320 bacterial reads remained (Table 2**).**

161

162 **Round II of 16S rRNA amplicon sequencing: Optimization**

163 Due to the severe host contamination observed in Round I that used the universal 16S
164 rRNA gene primers, we evaluated the performance of different 16S rRNA gene
165 primers with blockers (3' modified oligonucleotides with C3 spacer) that could
166 prevent the amplification of tomato chloroplast and mitochondrial rRNA genes (20-

167 22).
168
169 Based on the alignment of bacterial, tomato chloroplast and mitochondrial 16S rRNA
170 gene sequences (Fig. S1), we designed the primer sets and cognate blockers against
171 different variable region in 16S rRNA genes (Table S1 and S2). The new primer sets
172 and blockers were tested using the three WT-induced crown gall DNA samples from
173 Round I. After sequencing and data processing, the result indicated that the blockers
174 have variable effectiveness in reducing host contaminations (Table 3 and Fig. 2A**).**
175 For V3-4 and V5-7 primer sets, adding blockers increased the bacterial reads to 5.3-
176 41.5% of total reads, compared to only 0.2 -1.9% of bacterial reads per sample
177 without blockers. For V1-3 and V6-8 primer sets, adding blockers only increased the
178 bacterial reads to 1.6-5.6% of total reads per sample. The alpha rarefaction curves
179 based on the counts of operational taxonomic units (OTUs) indicated that, for those
180 crown gall samples, the curves would approach saturation when the sequencing depth
181 was over about 10,000 reads per sample (Fig. 2B). According to the bar plot of
182 bacterial composition at family levels, we could observe higher number of families
183 identified from the same crown galls amplified by adding blockers (Fig. 3A).
184 However, the result of Principal Coordinate Analysis (PCoA) indicated that adding
185 blockers did not cause significant biases in the inferred microbiota composition (Fig.
186 3B). However, the use of different primer sets resulted in significant difference in the
187 inferred microbiota composition (Fig. 3B, 3C), which has been reported previously
188 (23).

189 Overall, adding blockers at the PCR step increased bacterial read counts and the
190 resolution of gallobiome. Because the use of V5-7 primers and cognate blockers
191 obtained the highest number and percentage of bacterial reads, V5-7 set-up with
192 blockers were selected for 16 rRNA gene amplicon sequencing of crown galls
193 induced by WT and T6SS mutants.
194
195 **Round III of 16S rRNA amplicon sequencing: Impact of T6SS on gallobiome**
196 Among all of 139 crown galls collected, 53 tumors in the range of 0.06 – 0.56 g (24
197 induced by WT, 16 by Δ*tssL,* and 13 by Δ*tssB*) were used for the analysis. We
198 obtained an average of 6,9980 ± 26,452 (mean ± SD) reads per sample, ranged from
199 9,814 to 116,072 reads per sample. Before the analysis, the amplicon sequence

200 variants (ASVs) were clustered into 99% OTUs and the singletons were removed.
201 Based on the alpha rarefaction curves and the minimal read counts of the samples we
202 got (Fig. S2), diversity analysis was conducted with datasets subsampling at 9800
203 reads per sample. The result of PCoA showed that the gallobiome induced by WT and
204 two T6SS mutant strains were not significantly different (Fig. 4A). Most of the
205 variation between samples were contributed by different seasons (July vs.
206 October/November) (Fig. 4B). After splitting and re-analyzing the dataset based on
207 the month of inoculation, we observed the difference between the gallobiomes
208 associated with WT and two T6SS mutants in July (Fig. 4C). In contrast, no
209 difference was detected in those galls induced in October or November (Fig. 4D and
210 4E).
211
212 The alpha diversity indices including observed OTUs, Shannon index, and Pielou's
213 evenness index had no significant difference between the gallobiomes associated with
214 WT and T6SS mutants (Fig. 5A, 5B and 5C). Interestingly, we found that, in galls
215 induced in July, the WT gallobiome showed significantly higher Faith's phylogenic
216 diversity than the gallobiome associated with Δ*tssL*; and in galls induced in
217 November, the Δ*tssL* gallobiome showed higher diversity than the WT gallobiome
218 (Fig. 5D). The gallobiome associated with Δ*tssB* also exhibited higher diversity than
219 the WT gallobiome but the difference was not statistically significant.
220 While there were variations in bacterial compositions among crown galls, the top 10
221 bacterial family in gallobiomes were quite consistent, including: Rhizobiaceae,
222 Comamonadaceae, Chitinophagaceae, Methyphliaceae, Caulobacteraceae,
223 Sphingomonadaceae, Microbacreriaceae, Xanthobacteraceae, Oxalobacteraceae, and
224 Pseudomonaceae (Fig. 5E). The bacterial family Rhizobiaceae, which *A. tumefaciens*
225 belongs to, was found to be highly variable and accounted for 5-85% of the entire
226 community. The most abundant OTU in this Rhizobiaceae dataset was 100% matched
227 to 16S rRNA genes of *A. tumefaciens* C58, suggesting that the abundance of this OTU
228 likely indicated to the relative abundance of *A. tumefaciens* WT or mutant inoculum
229 in crown galls. When the weight of crown galls was plotted against the relative
230 abundance of this OTU in gallobiomes, we found that the abundance of Rhizobiaceae
231 in July was dramatically lower than those in October and November (Fig. 5F), but
232 there was no significant difference observed among different strains. Furthermore, a

233 positive correlation between weight of crown galls and relative abundance of *A.*
234 *tumefaciens* OTU was observed (Fig. 5G).
235
236 **Sphingomonadaceae and Burkholderiacea were more abundant in the**
237 **gallobiomes induced by the T6SS mutants in July**
238 Next, we analyzed the species-level OTU and family with differential abundance
239 (DA) between gallobiome associated with WT and T6SS mutants in July. Two OTUs
240 belonged to Sphingomonadaceae, named as SphinOTU1 and SphinOTU2 here, and
241 Burkhoderiaceae family were significantly enriched in the gallobiomes induced by
242 T6SS mutants (Fig. 6A). SphinOTU1 was only present in gallobiomes in July but not
243 in October/November, and SpinOTU2 was present in both July and October but not in
244 November (Fig 6B). Neither SpinOTU1 or SpinOTU2 was identified in gallobiomes
245 induced by the WT in July. Burkhoderiaceae was enriched in gallobiomes induced by
246 the T6SS mutants in July, but no consistent enrichment in October and November
247 (**Fig 6C**). Although SphinOTU1 and SphinOTU2 were only present in gallobiomes
248 induced by T6SS mutants in July; at family level, Sphingomonadaceae was not
249 enriched in T6SS-dependent manner in any months (Fig. 6C).
250
251 ***A. tumefaciens* exhibits T6SS antagonism to a *Sphingomonas* sp. isolate**
252 The T6SS-dependent differential abundance of two *Sphingomonas* OTUs in
253 gallobiomes motivated us to investigate whether *A. tumefaciens* exhibits T6SS
254 antibacterial activity to *Sphingomonas.* A *Sphingomonas* sp. strain R1 isolated from
255 the tomato rhizosphere in one soil inoculation experiment was used for *in vitro* and *in*
256 *planta* interbacterial competition assays. The results showed that the colony forming
257 unit (CFU) of *Sphingomonas* sp. R1 was lower after co-culture with *A. tumefaciens*
258 C58 WT than with T6SS mutants (Fig. 7A**)**. Each of *A. tumefaciens* C58 strains was
259 also mixed at 1:1 ratio with *Sphingomonas* sp. R1 to determine their colonization
260 efficiency and occupation by counting CFU from wounded tomato stems and crown
261 galls by soil inoculation. The results showed a reduced colonization efficiency of
262 *Sphingomonas* sp. R1 when co-inoculated with WT as compared to that with Δ*tssL*
263 and Δ*tssB* or R1 only, although not statistically different between WT and T6SS
264 mutants (Fig. 7B). No difference on the recovered CFU among *A. tumefaciens* WT
265 and T6SS mutants inoculated alone or with *Sphingomonas* sp. R1. However, we

266 noticed that the colonization efficiency of those T6SS mutants was more variable as
267 compared to those of WT from the combined data set (Fig. 7C). Surprisingly,
268 *Sphingomonas* sp. R1 was not always present in crown galls at 28 day-post-
269 inoculation (dpi), in which R1 was only recovered from one out of three independent
270 experiments (Fig. S3). The abundance of *A. tumefaciens* C58 ranged from 10^4 to 10^7
271 CFU per gall and no consistent difference could be observed between the WT and the
272 T6SS mutants. Together, these results suggest that *A. tumefaciens* C58 exhibits weak
273 but detectable antibacterial activity to inhibit the *in vitro* growth and plant
274 colonization efficiency of *Sphingomonas* sp. R1. The T6SS may help *A. tumefaciens*
275 to maintain stable colonization on plant surface for effective infection, leading to
276 higher disease incidence.
277

278 **DISCUSSION**

279 In this study, we designed experiments to address whether T6SS affects *Agrobacterium*
280 tumorigenesis and gallobiome. By establishing a soil inoculation platform to evaluate
281 the disease incidence of *A. tumefaciens* on wounded stems of tomato seedlings across
282 seasons, we revealed that T6SS exhibits positive impact on stable colonization and
283 disease occurrence efficiency but no impacts on tumor weight. Furthermore, by
284 developing an effective protocol named as Blocker-mediated Bacterial 16S rRNA gene
285 amplicon Enrichment Sequencing (BBRES) that minimizes host contamination, we
286 found that seasons or environmental factors, but not T6SS are the major driver in
287 shaping gallobiome compositions.
288

289 The evidences that *A. tumefaciens* T6SS promotes tumorigenesis by soil inoculation
290 (Table 1, Fig. 1) but not under direct inoculation on tomato stems (19) suggest that the
291 T6SS is not directly involved in virulence. Instead, *A. tumefaciens* deploys its
292 antibacterial activity to increase the occurrence of infection in the presence of relatively
293 complex microbial communities in soil or rhizosphere. Once the tumor is induced,

294 T6SS is not required for tumor development since no significant tumor weight was
295 observed between WT and T6SS mutants (Fig. 1B). The presence of T6SS has no
296 impact on the population size of agrobacteria, consistent with a recent study that T6SS
297 genes were not identified as fitness genes by Tn-seq screen in crown galls (24). The
298 T6SS of *A. tumefaciens* C58 also appears not the key factor to shape or maintain the
299 gallobiome, suggesting that *A. tumefaciens* may use other ways for niche competition
300 in the tumors. It is generally believed that the agrobacterial strain inciting tumors and
301 later become residents of its population have privilege to access the specific opines
302 synthesized by its T-DNA (25). This "opine concept" has not been experimentally
303 validated but recent study showed that the ability of agrobacteria to trap opines can
304 acquire a competitive advantage over the siblings which cannot utilize opine (26).
305 Therefore, it would be interesting to investigate whether opine synthesis and other
306 fitness genes would impact the crown gall microbiota in which T6SS may
307 synergistically enhance the niche occupation.
308
309 The findings that disease incidence and crown gall weight in reverse correlation
310 with temperature (Fig. 1C) are expected. Early studies demonstrated that crown gall
311 tumor sizes were dramatically decreased when the host plants were inoculated at 28-
312 30°C, with no galls were formed at 31°C or above (27, 28). In addition, VirB/D4
313 T4SS complex and its associated T-pilus are more stable or produced at higher levels
314 at 19°C than 28°C whereas T4SS-mediated plasmid conjugation is deficient at 28°C
315 (29-33). The increased tumor weight when inoculated in fall/winter is also correlated
316 with a higher relative abundance of agrobacterial OTU (Fig. 5G), suggesting the
317 active proliferation of agrobacterial population inside crown galls. Furthermore, our
318 data showed that crown galls produced in summer have distinct microbiota as
319 compared to those from fall/winter (Fig. 4B), which echoes previous studies on

320 *Agrobacterium vitis* that crown gall microbiota of grapevine is significantly different
321 in summer (34). Interestingly, while there is no global difference of gallobiome
322 induced by WT or T6SS mutants inoculated in fall/winter, we found that the two
323 *Sphingomonas* OTUs and the family Burkholderiaceae were only present or
324 significantly enriched in the gallobiome induced by T6SS mutants in summer (Fig. 6).
325 By counting viable agrobacterial inoculum, we showed the *A. tumefaciens* exhibits a
326 T6SS-mediated antibacterial activity to *Sphingomonas* sp. R1 *in vitro* and in
327 rhizosphere (Fig. 7A, B) but no significant difference of R1 abundance between the
328 tumors co-infected with *A. tumefaciens* WT or T6SS mutants (Fig. S3). Accordingly,
329 we also observed more stable colonization of *A. tumefaciens* WT than T6SS mutants
330 on wounded tomato stems via soil inoculation (Fig. 7C). To this end, it remains to be
331 determined whether the absence or reduced abundance of *Sphingomonas* and
332 Burkholderiaceae of gallobiome induced by WT as compared to those by T6SS
333 mutants are due to antibacterial activity conferred by WT T6SS. However, current
334 evidence suggests that *A. tumefaciens* may use T6SS to gain competitive advantage
335 by its antibacterial activity against other bacterial species residing in the soil or
336 rhizosphere and therefore increases its success in inciting tumors on infected plants.
337
338 Besides Rhizobiaceae that agrobacteria belong to, other bacterial families were also
339 occupied considerable proportions of crown gall microbiota, such as
340 Comamonadaceae, members of which are commonly found in soil and water as well
341 as plant-associated bacteria *Variovorax* shown to be important for root growth of
342 *Arabidopsis* (35, 36). Bacteria belong to Xanthobacteraceae and Pseudomonaceae, the
343 two families highly associated with plants as either pathogens or commensals, also
344 had high relative abundance in the crown galls. Some *Pseudomonas* species such as *P.*
345 *fluorescens* and *P. putida* are capable to utilize opine (37, 38), which may explain why

346 bacterial species other than the agrobacterial inoculum could also colonize and
347 propagate in high relative abundance in crown galls.
348
349 We found that the predominance of plant DNA in crown gall samples led to the low
350 resolution of endophytic bacterial microbiota survey via standard 16S rRNA gene
351 amplicon sequencing due to the co-amplification of chloroplast and mitochondrial
352 sequences. Although the use of 16S rRNA gene primers containing mismatches to 16S
353 rRNA gene of plant chloroplast or mitochondria could potentially reduce host
354 contamination in endophytic microbiota studies (23, 39), the "bacteria-specific"
355 primers did not work well in previous studies (20) and resulted in > 90% host reads of
356 our initial attempt (Round I) (Table 2). When adding blockers that could specifically
357 anneal to chloroplast or mitochondrial DNA but not be extended by DNA polymerase
358 during PCR, we successfully reduced the host contamination and obtained sufficient
359 sequencing depth for this study. Our results support the effectiveness of blockers in
360 increasing bacterial reads of endophyte community (20-22). The newly developed
361 BBRES protocol for gallobiome may be applicable to microbiota associated with
362 tomato, or even other plants after modifying the blocker sequences.
363
364 To date, collective plant microbiota studies suggest the enrichment of T6SS genes in
365 microbiota and as a protected trait for niche competition in microbiota (5, 8).
366 However, the role and impact of T6SS in different plant and microbiome contexts
367 may be different. Our study suggest that agrobacteria may use T6SS to gain
368 competitive advantage at initial stage of infection but likely not critical for its
369 proliferation once they established their niche inside the crown galls. Future work to
370 investigate the spatial distribution of agrobacterial cells and other endophytes inside
371 crown gall or wounded site of plants together with visualization of T6SS dynamics is

372 important to dissect the role of T6SS during agrobacterial life cycle.

373

374 **MATERIALS AND METHODS**

375 **Bacterial strains and growth condition**

376 Bacterial strains and plasmids used in this study are listed in Table S3. *Agrobacterium*
377 *tumefaciens* strain C58 wild type and two T6SS mutants (i.e., Δ*tssB* and Δ*tssL*) (40)
378 were first streaked on 523 medium agar plates (41) and incubate at 25 °C for 48 hr.
379 *Sphingomonas* sp. R1 was grown on R2A medium without soluble starch and
380 pyruvate (42). *Escherichia coli* was grown on lysogeny broth (LB) medium at 37°C.
381 Freshly grown colony was inoculated into corresponding broth for overnight culture.
382 The antibiotics and concentration used are: 10 μg/ml gentamycin for *E. coli,* 50 μg/ml
383 gentamycin for *A. tumefaciens*, and 20 μg/ml kanamycin and 50μg/ml gentamycin for
384 *Sphingomonas* sp. R1.

385

386 **Construction of strains enable antibiotics selection**

387 Primers used for construction are listed in Table S4. The DNA fragment containing
388 gentamycin resistance (Gm^R) gene and green fluorescence protein *gfp*(S65T) were
389 amplified from pRL662::GFP(S65T) with the primer pair "BclI-GFP-GmR-F-25" and
390 "BclI-GFP-GmR-R-25", and then cloned into XbaI digested pJQ-COM. The newly
391 constructed plasmid was named pJQ-com-GmR-GFP, which enabled the generation of
392 Gm^R gene and *gfp* (S65T) knocked in at the upstream of *actC* (*atu5330*) of *A.*
393 *tumefaciens* genome after double crossover. The knock-in strains were generated in *A.*
394 *tumefaciens* C58, Δ*tssB*, and Δ*tssL* background. The knock-in event and excision of
395 pJQ200ks backbone were confirmed by GFP signal, gentamycin resistance, and PCR
396 with the primer pair "3'sacB-5'GmR pJQ200 F" and "3'sacB-5'GmR pJQ200 R",
397 which target the fragment between *sacB* and Gm^R gene on pJQ200ks. The plasmids
398 pRL66::GFP(S65T) and pBBR::mCherry conferring kanamycin resistance were each
399 transformed into *Sphingomonas* sp. R1 through electroporation. The procedure of
400 electroporation, doble crossover via pJQ200ks were performed as described
401 previously (43).

402

403 **Plant material and growth condition**

404 Seeds of *Solanum lycopersicum* (tomato) cultivar Known-You 301 from KNOWN-
405 YOU SEED CO., LTD (Kaohsiung, Taiwan) were germinated and grown in
406 unsterilized potting mixture (Jiffy® Premium Fine Peat Substrate, perlite, and
407 vermiculite, mixed in 4:1:1 ratio, v:v:v) in the greenhouse EL329
408 (N25.043047890856812, E121.61135464167913, Greenhouse building, Academia
409 Sinica, Taipei, Taiwan).
410
411 **Soil inoculation**
412 Soil inoculation method was performed essentially following the method used for *A.*
413 *tumefaciens* on pea and walnut (44, 45). Overnight (14-16 hr) culture of *A.*
414 *tumefaciens* strain in 12 ml of 523 broth were centrifugated at 6,000 × g for 10 min.
415 The pellets were washed once by using 10 ml of sterile saline (0.9% NaCl in H_2O).
416 The washed pellets were centrifuged and resuspended in sterile saline with OD_{600}
417 adjusted to 1. Bacterial suspension was mixed into unsterilized soil (1 ml suspension
418 per 100 g of soil), which is expected to result in ~10^7 colony-forming units (CFUs)/g
419 soil. Tomato seedlings with two true leaves (two- to three-week-old) were wounded at
420 the site between primary root and cotyledons by a fire-sterilized sewing needle,
421 planted into the inoculated soil, and grown in the greenhouse. Each strain was
422 inoculated with 14 to 20 tomato seedlings, and the inoculation with saline were used
423 as a negative control
424
425 **Harvest, surface sterilization and storage of crown gall samples**
426 Two months after the inoculation, tomato plants were harvested to examine gall
427 formation on the wounded site. The disease incidence was calculated by dividing the
428 number of plants with visible gall formation by the total number of inoculated plants.
429 The sections with crown gall were cut out and sterilized in 35 ml of sterilization
430 solution (3% NaOCl, 0.01% tween-20) for 30s, then transferred to 35 ml of 70%
431 ethanol and washed in 35 ml of sterile H_2O for three times (46). The sterilization was
432 evaluated by spreading 100 µl liquid from the third wash onto 523 agar plate for 2
433 days to make sure that there was no growth of bacteria. After sterilization, the crown
434 galls were dissected from each of the plant segments in sterile petri dish, wrapped in
435 sterile aluminum foil, frozen by liquid nitrogen, and stored at -80 °C prior to DNA
436 extraction.

437

438 **DNA extraction form crown galls**

439 Crown gall samples were homogenized by pestle and mortar with liquid nitrogen.
440 0.25 g of homogenized tissue were transferred to the beating tube of DNeasy®
441 PowerSoil® Kit (Qiagen, Germany) following the manufacturer's instructions.
442 Concentrations of extracted DNA were determined by NanoDrop™ 1000 (Thermo
443 Fisher Scientific, United State) and Qubit dsDNA HS (Invitrogen, United State).

444

445 **16S rRNA gene amplification and sequencing**

446 Three rounds of amplicon sequencing were conducted in this study. The round I was
447 conducted according to established protocols of soil microbiota studies using 16S
448 rRNA gene variable regions (23). Each primer with a partial adaptor sequence was
449 compatible to Illumina Truseq Combinatorial dual (CD) index system. The first PCR
450 amplifications were carried out in following 25 µl reaction: 5 ng DNA template, 2×
451 KAPA HiFi HotStart DNA Polymerase ReadyMix (Roche, Switzerland), and 0.2 µM
452 for each of the forward and reverse primers. The first PCR program and reaction
453 details for V3-4 and V5-7 are listed in **Table S5**. The PCR products were purified by
454 Ampure XP beads (Thermo Fisher Scientific Inc, Sweden). The V5-7 PCR products
455 underwent BluePippin (Sage Science) size-selection to remove tomato amplicon. To
456 attach dual indices and full-length Illumina sequencing adapters, a second round of
457 PCR amplifications were employed for 50 µl reactions with purified or size-selection
458 PCR products, 2× KAPA HiFi HotStart DNA Polymerase ReadyMix (Roche,
459 Switzerland), and 0.5 µM for each of the forward and reverse primers. All the library
460 products of second PCR were purified and pooled. Pooled libraries were loaded onto
461 an Illumina MiSeq V3 flow cell (Illumina, United States) and for 2×300 bp paired-
462 end sequencing.

463

464 The round II of amplicon sequencing was conducted to test the effect of adding PCR
465 blockers on reducing plant chloroplast and mitochondrial sequences. Three gall
466 samples (1115-W21, 1115-W22 and 1115-W25) were used as the DNA templates to
467 provide biological replicates. For each DNA sample, four primer pairs targeting
468 different variable regions of 16S rRNA gene were used, including: V1-3, V3-4, V5-7,
469 and V6-8 (Table S1). Each primer contained a partial adaptor sequence of the Illumina

470 Truseq Combinatorial dual (CD) index system. Cognate 3' C3 spacer modified
471 oligonucleotides (blockers) which would block the amplification of 16S rRNA genes
472 of tomato chloroplasts and mitochondria were designed according to a previous study
473 (20) and applied to one of the two PCRs for each sample-primer combination (Table
474 S2). Procedures for PCR and Illumina sequencing were based on those used for round
475 I, but the amount of DNA template was increased to 25 ng to reduce PCR cycle time
476 and the annealing temperature was adjusted for blockers. More detailed technical
477 information is provided in Table S4.
478
479 Based on results from the first two rounds of amplicon sequencing, an optimized
480 protocol that utilizes blockers and targets V5-7 regions was used for round III. All 53
481 crown gall samples were included in this final round.
482
483 **Raw read processing and microbiota analysis**
484 The Illumina raw reads in FASTQ format were imported into QIIME2 release 2020.8
485 (47). The primer region of imported sequences was trimmed using DADA2 (48). The
486 denoised and merged paired-end reads were used to construct output feature tables
487 containing amplicon sequence variants (ASVs) ID and counts in different samples.
488 For amplicon sequencing round III, the ASVs were further clustered into operational
489 taxonomic units (OTUs) based on 99% sequence identity using the "qiime vsearch
490 cluster-features-de-novo" function (49) and the singletons were removed by using the
491 "qiime feature-table filter-features" function prior to the downstream analysis. The
492 taxonomic information was inferred for representative OTU sequences via pre-trained
493 q2-feature-classifier (50) and classify-sklearn naïve Bayes classifier based on SILVA
494 version 138 SSU Ref NR 99 full-length sequences dataset (51). The sequences
495 assigned as chloroplasts, mitochondria, eukaryotes, archaea, or unknown were
496 removed. After the filtering, a phylogenetic tree of eubacterial sequences was inferred
497 using the q2-fragment-insertion plug-in (52-55) based on the SILVA 128 SEPP
498 reference database. Weighted Unifrac (56) analysis of those datasets was performed
499 based on insertion tree; the distance matrix and principal coordinate analysis (PCoA)
500 plot were generated using QIIME2. For round III, phylogenic and diversity analysis
501 was conducted using "qiime diversity core-metrics-phylogenetic" and the sub-
502 sampling depth was set to 9,800 reads/sample.

503

504 **Differential abundance analysis of OTU**

505 Analysis of composition of microbiomes (ANCOM) was applied to identify OTUs
506 that have significantly different relative abundance in the gallobiome associated with
507 *A. tumefaciens* C58 WT and T6SS-dificient mutants using the function "qiime
508 composition ancom" in QIIME2. The feature table collapsed into family level was
509 imported and transformed by centred log-ratio transformation. The null hypothesis of
510 ANCOM is that the abundance of two OTUs were not different between two study
511 groups. After performing all comparison between each OTU in two study groups, the
512 times that the null hypothesis was rejected is called *w*. OTUs having *w* values that are
513 at 70 percentile or higher are considered as significant (57, 58).

514

515 **Interbacterial competition assay *in vitro* and *in planta***

516 For interbacterial competition *in vitro,* the bacterial suspension was adjusted to OD_{600}
517 equals to 3.0 in 0.9% NaCl (w/v) after overnight culture. For the *in vitro* competition,
518 the attacker strains (*A. tumefaciens* C58 WT, Δ*tssL* or Δ*tssB*) were further diluted into
519 OD_{600} equals to 1, and the prey *Sphingomonas* sp. R1 containing pRL662::GFP was
520 further diluted into OD_{600} equal to 0.3 or 0.1 for mixing with the attacker in equal
521 volume for different density ratio. Two spots of 10 µl mixture were spotted on
522 *Agrobacterium* kill-triggering medium(18). After co-incubated for 16 h in 25 °C, the
523 colonies were scraped and resuspended in 1 ml 0.9% NaCl (w/v), and spread via
524 exponential mode of easySpiral Dilute® (Ref. 414 000, INTERSCIENCE, France) on
525 523 media containing 30 µg/ml gentamycin to recover the prey.

526 For *A. tumefaciens* colonization with or without *Sphingomonas* sp. R1, each of *A.*
527 *tumefaciens* C58 strains (WT, Δ*tssL* or Δ*tssB*) with Gm^R-GFP knock-in was mixed
528 with *Sphingomonas* sp. R1 containing pBBR::mCherry at equal OD_{600} =1.0. The 5 µl
529 mixture was inoculated on the needle-wounded stem of tomato seedling with first pair
530 of true leaves. Tomato seedlings were harvested at 10 days post-inoculation (dpi). For
531 each plant, the 1 cm wounded segment was cut and rinsed by sterile water before

532 being transferred into a sterilized Eppendorf tube containing 1 ml of 0.9% NaCl. After
533 vortex at max speed for 3 minutes, the liquid was considered as the rhizosphere
534 sample. The samples were diluted and plated on media with gentamycin for CFU
535 calculation.

536 When counting the CFU of *A. tumefaciens* C58 and *Sphingomonas* sp. R1 in the
537 tumor, the crown galls were collected after growing in the greenhouse for three
538 weeks. The 1-cm tomato stem section containing the gall in middle was cut and
539 homogenized with 1 ml 0.9% NaCl (w/v) by sterilized mortar and pestle. The
540 homogenized tissue was diluted 10-fold and spread via exponential mode of
541 easySpiral Dilute® on 523 media containing 50 ppm gentamycin to recover the
542 attacker and prey. After incubation for two days at 25°C, the colonies were counted
543 by using the Scan® 500 Automatic colony counter (Ref 436 000, INTERSCIENCE,
544 France; software version 8.6.1) to calculate CFUs.

545 **Statistics and visualization**

546 GraphPad Prism 8 was used to perform t-test on sequencing read counts, one-way
547 ANOVA on CFU counts, two-way ANOVA followed by Turkey's multiple
548 comparison test on crown gall disease incidence and alpha diversity index, Kruskai-
549 Wallis test on tumor weight, Spearman correlation on gall weight and relative
550 abundance of *A. tumefaciens* OTU. The alpha-rarefaction curves were plotted using
551 Phyloseq (59) in R version 3.6.2. ADONIS in "qiime diversity beta-group-
552 significance" of QIIME2 (60, 61) was used to test if groups of samples have
553 significantly different microbiota composition. The taxonomic composition plots were
554 generated using qiime2R (v0.99.35, https://github.com/jbisanz/qiime2R) in R studio
555 2.
556

557 **DATA AVAILABILITY**

558 All raw data sets are available in the National Center for Biotechnology Information
559 (NCBI) under BioProject accession PRJNA894311.
560

561 **AUTHOR CONTRIBUTION**

562 Conceptualization: SCW, CHK, EML
563 Funding acquisition: CHK, EML

Investigation: SCW, CHK, EML
Methodology: SCW, APC, SJC, CHK
Project administration: EML
Supervision: CHK, EML
Validation: SCW, CHK
Visualization: SCW, CHK
Writing – original draft: SCW, CHK, EML
Writing – review & editing: SCW, APC, SJC, CHK, EML

ACKNOWLEDGEMENTS

The authors thank the members of Lai and Kuo labs for helpful discussion. We also acknowledge Lay-Sun Ma for constructing pRL662::GFP(S65T) and Stanton Gelvin for providing pBBR::mCherry. The Illumina sequencing library preparation was carried out in the Genomic Technology Core (Institute of Plant and Microbial Biology, Academia Sinica). We thank the Illumina MiSeq sequencing service provided by the Genomics Core (Institute of Molecular Biology, Academia Sinica).

FUNDING

Research in the Lai lab was supported by Institute of Plant and Microbial Biology, Academia Sinica, Academia Sinica and Academia Sinica Investigator Award to EML (grant no. AS-IA-107-L01). Research in the Kuo lab was supported by Academia Sinica and the Ministry of Science and Technology of Taiwan (MOST 109-2628-B-001-012; 110-2628-B-001-020; 111-2628-B-001-019). The funders had no role in study design, data collection and interpretation, or the decision to submit the work for publication.

REFERENCES

1. Coulthurst S. 2019. The Type VI secretion system: a versatile bacterial weapon. Microbiology (Reading) 165:503-515.
2. Jurenas D, Journet L. 2021. Activity, delivery, and diversity of Type VI secretion effectors. Mol Microbiol 115:383-394.
3. Lien YW, Lai EM. 2017. Type VI Secretion Effectors: Methodologies and Biology. Front Cell Infect Microbiol 7:254.
4. Gallegos-Monterrosa R, Coulthurst SJ. 2021. The ecological impact of a bacterial weapon: microbial interactions and the Type VI secretion system. FEMS Microbiol Rev 45.
5. Bulgarelli D, Garrido-Oter R, Munch PC, Weiman A, Droge J, Pan Y, McHardy AC, Schulze-Lefert P. 2015. Structure and function of the bacterial root

602 microbiota in wild and domesticated barley. Cell Host Microbe 17:392-403.
603 6. Wexler AG, Bao Y, Whitney JC, Bobay LM, Xavier JB, Schofield WB, Barry NA,
604 Russell AB, Tran BQ, Goo YA, Goodlett DR, Ochman H, Mougous JD, Goodman
605 AL. 2016. Human symbionts inject and neutralize antibacterial toxins to
606 persist in the gut. Proc Natl Acad Sci U S A 113:3639-44.
607 7. Verster AJ, Ross BD, Radey MC, Bao Y, Goodman AL, Mougous JD, Borenstein
608 E. 2017. The Landscape of Type VI Secretion across Human Gut Microbiomes
609 Reveals Its Role in Community Composition. Cell Host Microbe 22:411-419
610 e4.
611 8. Vogel CM, Potthoff DB, Schafer M, Barandun N, Vorholt JA. 2021. Protective
612 role of the Arabidopsis leaf microbiota against a bacterial pathogen. Nat
613 Microbiol 6:1537-1548.
614 9. Serapio-Palacios A, Woodward SE, Vogt SL, Deng W, Creus-Cuadros A, Huus
615 KE, Cirstea M, Gerrie M, Barcik W, Yu H, Finlay BB. 2022. Type VI secretion
616 systems of pathogenic and commensal bacteria mediate niche occupancy in
617 the gut. Cell Rep 39:110731.
618 10. Ma LS, Hachani A, Lin JS, Filloux A, Lai EM. 2014. *Agrobacterium tumefaciens*
619 deploys a superfamily of type VI secretion DNase effectors as weapons for
620 interbacterial competition in planta. Cell Host Microbe 16:94-104.
621 11. Bernal P, Allsopp LP, Filloux A, Llamas MA. 2017. The *Pseudomonas putida*
622 T6SS is a plant warden against phytopathogens. ISME J 11:972-987.
623 12. Bernal P, Llamas MA, Filloux A. 2018. Type VI secretion systems in plant-
624 associated bacteria. Environ Microbiol 20:1-15.
625 13. Vacheron J, Pechy-Tarr M, Brochet S, Heiman CM, Stojiljkovic M, Maurhofer
626 M, Keel C. 2019. T6SS contributes to gut microbiome invasion and killing of an
627 herbivorous pest insect by plant-beneficial *Pseudomonas protegens*. ISME J
628 13:1318-1329.
629 14. Hwang HH, Yu M, Lai EM. 2017. *Agrobacterium*-Mediated Plant
630 Transformation: Biology and Applications, vol 15. American Society of Plant
631 Biologists.
632 15. Wu CF, Santos MNM, Cho ST, Chang HH, Tsai YM, Smith DA, Kuo CH, Chang JH,
633 Lai EM. 2019. Plant-Pathogenic *Agrobacterium tumefaciens* Strains Have
634 Diverse Type VI Effector-Immunity Pairs and Vary in In-Planta
635 Competitiveness. Molecular Plant-Microbe Interactions 32:961-971.
636 16. Wu CF, Weisberg AJ, Davis EW, 2nd, Chou L, Khan S, Lai EM, Kuo CH, Chang JH.
637 2021. Diversification of the Type VI Secretion System in Agrobacteria. mBio
638 12:e0192721.
639 17. Chou L, Lin YC, Haryono M, Santos MNM, Cho ST, Weisberg AJ, Wu CF, Chang

640 JH, Lai EM, Kuo CH. 2022. Modular evolution of secretion systems and
641 virulence plasmids in a bacterial species complex. BMC Biol 20:16.
642 18. Yu M, Wang YC, Huang CJ, Ma LS, Lai EM. 2020. *Agrobacterium tumefaciens*
643 Deploys a Versatile Antibacterial Strategy to Increase its Competitiveness. J
644 Bacteriol doi:10.1128/JB.00490-20.
645 19. Wu HY, Chung PC, Shih HW, Wen SR, Lai EM. 2008. Secretome Analysis
646 Uncovers an Hcp-Family Protein Secreted via a Type VI Secretion System in
647 *Agrobacterium tumefaciens*. J Bacteriol 190:2841-2850.
648 20. Lefevre E, Gardner CM, Gunsch CK. 2020. A novel PCR-clamping assay
649 reducing plant host DNA amplification significantly improves prokaryotic
650 endo-microbiome community characterization. Fems Microbiology Ecology
651 96.
652 21. Fitzpatrick CR, Lu-Irving P, Copeland J, Guttman DS, Wang PW, Baltrus DA,
653 Dlugosch KM, Johnson MTJ. 2018. Chloroplast sequence variation and the
654 efficacy of peptide nucleic acids for blocking host amplification in plant
655 microbiome studies. Microbiome 6:144.
656 22. Arenz BE, Schlatter DC, Bradeen JM, Kinkel LL. 2015. Blocking primers reduce
657 co-amplification of plant DNA when studying bacterial endophyte
658 communities. Journal of Microbiological Methods 117:1-3.
659 23. Thijs S, Op De Beeck M, Beckers B, Truyens S, Stevens V, Van Hamme JD,
660 Weyens N, Vangronsveld J. 2017. Comparative Evaluation of Four Bacteria-
661 Specific Primer Pairs for 16S rRNA Gene Surveys. Front Microbiol 8:494.
662 24. Torres M, Jiquel A, Jeanne E, Naquin D, Dessaux Y, Faure D. 2022.
663 *Agrobacterium tumefaciens* fitness genes involved in the colonization of plant
664 tumors and roots. New Phytol 233:905-918.
665 25. Guyon P, Chilton MD, Petit A, Tempe J. 1980. Agropine in "null-type" crown
666 gall tumors: Evidence for generality of the opine concept. Proc Natl Acad Sci U
667 S A 77:2693-7.
668 26. Lang J, Vigouroux A, Planamente S, El Sahili A, Blin P, Aumont-Nicaise M,
669 Dessaux Y, Morera S, Faure D. 2014. *Agrobacterium* uses a unique ligand-
670 binding mode for trapping opines and acquiring a competitive advantage in
671 the niche construction on plant host. PLoS Pathog 10:e1004444.
672 27. Riker AJ. 1926. Studies on the influence of some environmental factors on the
673 development of crown gall. Journal of Agricultural Research 32:0083-0096.
674 28. Braun AC. 1947. Thermal Studies on the Factors Responsible for Tumor
675 Initiation in Crown Gall. American Journal of Botany 34:234-240.
676 29. Fullner KJ, Nester EW. 1996. Temperature affects the T-DNA transfer
677 machinery of *Agrobacterium tumefaciens*. J Bacteriol 178:1498-504.

678 30. Fullner KJ, Lara JC, Nester EW. 1996. Pilus assembly by *Agrobacterium* T-DNA
679 transfer genes. Science 273:1107-9.
680 31. Lai EM, Kado CI. 1998. Processed VirB2 is the major subunit of the
681 promiscuous pilus of *Agrobacterium tumefaciens*. J Bacteriol 180:2711-7.
682 32. Lai EM, Kado CI. 2000. The T-pilus of *Agrobacterium tumefaciens*. Trends
683 Microbiol 8:361-9.
684 33. Baron C, Domke N, Beinhofer M, Hapfelmeier S. 2001. Elevated temperature
685 differentially affects virulence, VirB protein accumulation, and T-pilus
686 formation in different *Agrobacterium tumefaciens* and *Agrobacterium vitis*
687 strains. J Bacteriol 183:6852-61.
688 34. Faist H, Keller A, Hentschel U, Deeken R. 2016. Grapevine (Vitis vinifera)
689 Crown Galls Host Distinct Microbiota. Appl Environ Microbiol 82:5542-52.
690 35. Willems A, De Ley., J. , Gillis, M. Kersters, D. K. . 1991. Comamonadaceae, a
691 New Family Encompassing the *Acidovorans* rRNA Complex, Including
692 Variovoraxparadoxus gen. nov., comb. nov. for Alcaligenes paradoxus (Davis
693 1969). INTERNATIONJOAULRNAOLF SYSTEMATBICACTERIOLO 41.
694 36. Finkel OM, Salas-Gonzalez I, Castrillo G, Conway JM, Law TF, Teixeira P, Wilson
695 ED, Fitzpatrick CR, Jones CD, Dangl JL. 2020. A single bacterial genus
696 maintains root growth in a complex microbiome. Nature 587:103-108.
697 37. Moore LW, Chilton WS, Canfield ML. 1997. Diversity of opines and opine-
698 catabolizing bacteria isolated from naturally occurring crown gall tumors.
699 Applied and Environmental Microbiology 63:201-207.
700 38. Beauchamp CJ, Dion P, Kloepper JW, Antoun H. 1991. Physiological
701 Characterization of Opine-Utilizing Rhizobacteria for Traits Related to Plant
702 Growth-Promoting Activity. Plant and Soil 132:273-279.
703 39. Beckers B, Op De Beeck M, Thijs S, Truyens S, Weyens N, Boerjan W,
704 Vangronsveld J. 2016. Performance of 16s rDNA Primer Pairs in the Study of
705 Rhizosphere and Endosphere Bacterial Microbiomes in Metabarcoding
706 Studies. Front Microbiol 7:650.
707 40. Lin JS, Ma LS, Lai EM. 2013. Systematic Dissection of the *Agrobacterium* Type
708 VI Secretion System Reveals Machinery and Secreted Components for
709 Subcomplex Formation. PLoS One 8:e67647.
710 41. Kado CI, and Heskett, M.G. . 1970. Selective media for isolation of
711 *Agrobacterium, Carynebacterium, Erwinia, Pseudomonas,* and
712 *Xanthomonas*. . Phytopathology 60:969-976.
713 42. Massa S, Caruso M, Trovatelli F, Tosques M. 1998. Comparison of plate count
714 agar and R2A medium for enumeration of heterotrophic bacteria in natural
715 mineral water. World Journal of Microbiology & Biotechnology 14:727-730.

716 43. Ma LS, Lin JS, Lai EM. 2009. An IcmF family protein, ImpLM, is an integral
717 inner membrane protein interacting with ImpKL, and its walker a motif is
718 required for type VI secretion system-mediated Hcp secretion in
719 *Agrobacterium tumefaciens*. J Bacteriol 191:4316-29.
720 44. Hawes MC, Smith LY. 1989. Requirement for chemotaxis in pathogenicity of
721 *Agrobacterium tumefaciens* on roots of soil-grown pea plants. J Bacteriol
722 171:5668-71.
723 45. Yakabe LE, Parker SR, Kluepfel DA. 2012. Role of Systemic *Agrobacterium*
724 *tumefaciens* Populations in Crown Gall Incidence on the Walnut Hybrid
725 Rootstock 'Paradox'. Plant Disease 96:1415-1421.
726 46. McPherson MR, Wang P, Marsh EL, Mitchell RB, Schachtman DP. 2018.
727 Isolation and Analysis of Microbial Communities in Soil, Rhizosphere, and
728 Roots in Perennial Grass Experiments. Jove-Journal of Visualized Experiments
729 doi:ARTN e57932
730 10.3791/57932.
731 47. Bolyen E, Rideout JR, Dillon MR, Bokulich NA, Abnet CC, Al-Ghalith GA,
732 Alexander H, Alm EJ, Arumugam M, Asnicar F, Bai Y, Bisanz JE, Bittinger K,
733 Brejnrod A, Brislawn CJ, Brown CT, Callahan BJ, Caraballo-Rodriguez AM,
734 Chase J, Cope EK, Da Silva R, Diener C, Dorrestein PC, Douglas GM, Durall DM,
735 Duvallet C, Edwardson CF, Ernst M, Estaki M, Fouquier J, Gauglitz JM, Gibbons
736 SM, Gibson DL, Gonzalez A, Gorlick K, Guo J, Hillmann B, Holmes S, Holste H,
737 Huttenhower C, Huttley GA, Janssen S, Jarmusch AK, Jiang L, Kaehler BD, Kang
738 KB, Keefe CR, Keim P, Kelley ST, Knights D, et al. 2019. Reproducible,
739 interactive, scalable and extensible microbiome data science using QIIME 2.
740 Nat Biotechnol 37:852-857.
741 48. Callahan BJ, McMurdie PJ, Rosen MJ, Han AW, Johnson AJ, Holmes SP. 2016.
742 DADA2: High-resolution sample inference from Illumina amplicon data. Nat
743 Methods 13:581-3.
744 49. Rognes T, Flouri T, Nichols B, Quince C, Mahe F. 2016. VSEARCH: a versatile
745 open source tool for metagenomics. PeerJ 4:e2584.
746 50. Bokulich NA, Kaehler BD, Rideout JR, Dillon M, Bolyen E, Knight R, Huttley GA,
747 Gregory Caporaso J. 2018. Optimizing taxonomic classification of marker-gene
748 amplicon sequences with QIIME 2's q2-feature-classifier plugin. Microbiome
749 6:90.
750 51. Yilmaz P, Parfrey LW, Yarza P, Gerken J, Pruesse E, Quast C, Schweer T, Peplies
751 J, Ludwig W, Glockner FO. 2014. The SILVA and "All-species Living Tree Project
752 (LTP)" taxonomic frameworks. Nucleic Acids Res 42:D643-8.
753 52. Janssen S, McDonald D, Gonzalez A, Navas-Molina JA, Jiang L, Xu ZZ, Winker K,

754 Kado DM, Orwoll E, Manary M, Mirarab S, Knight R. 2018. Phylogenetic
755 Placement of Exact Amplicon Sequences Improves Associations with Clinical
756 Information. mSystems 3.
757 53. Matsen FA, Hoffman NG, Gallagher A, Stamatakis A. 2012. A format for
758 phylogenetic placements. PLoS One 7:e31009.
759 54. Eddy SR. 2011. Accelerated Profile HMM Searches. PLoS Comput Biol
760 7:e1002195.
761 55. Matsen FA, Kodner RB, Armbrust EV. 2010. pplacer: linear time maximum-
762 likelihood and Bayesian phylogenetic placement of sequences onto a fixed
763 reference tree. BMC Bioinformatics 11:538.
764 56. Lozupone C, Knight R. 2005. UniFrac: a new phylogenetic method for
765 comparing microbial communities. Appl Environ Microbiol 71:8228-35.
766 57. Lin H, Peddada SD. 2020. Analysis of microbial compositions: a review of
767 normalization and differential abundance analysis. NPJ Biofilms Microbiomes
768 6:60.
769 58. Mandal S, Van Treuren W, White RA, Eggesbo M, Knight R, Peddada SD. 2015.
770 Analysis of composition of microbiomes: a novel method for studying
771 microbial composition. Microb Ecol Health Dis 26:27663.
772 59. McMurdie PJ, Holmes S. 2013. phyloseq: an R package for reproducible
773 interactive analysis and graphics of microbiome census data. PLoS One
774 8:e61217.
775 60. Anderson MJ. 2001. A new method for non-parametric multivariate analysis
776 of variance. Austral Ecology 26:32-46.
777 61. Dixon P. 2003. VEGAN, a package of R functions for community ecology.
778 Journal of Vegetation Science 14:927-930.
779
780

781 **FIGURE LEGENDS**

782 **Figure 1. Tumorigenesis assay of *A. tumefaciens* C58 and its T6SS-deficienct**
783 **mutants.**

784 For each experiment, 14-20 wounded tomato seedlings were grown in soil containing
785 one of the strains tested (i.e., C58 WT, Δ*tssL*, and Δ*tssB*) and collected at 60 days post
786 inoculation (dpi). (A) Disease incidence plotted by strain and color-coded according
787 to the month of inoculation (light yellow, June; orange, July; light blue, October; dark
788 blue, November). Lines and error bars indicate mean ± SD. Statistical significance
789 was tested using two-way ANOVA followed by Tukey's multiple comparisons; p =
790 0.025 and 0.027 when comparing the wild type to Δ*tssL* and Δ*tssB*, respectively. (B)
791 Weight distribution of the galls collected. No significant difference among the three
792 strains (p = 0.15, Kruskai-Wallis test). (C) Correlation plot of disease incidence and
793 temperature of daily average. (D) Crown galls generated through soil inoculation,
794 example from inoculation on 11/15/2018. N indicated no gall formation in some of
795 inoculated plants.

796

797 **Figure 2. Optimizing 16S rRNA gene amplification by using PCR blockers.**

798 Three crown gall samples (named as 21W, 22W and 25W) induced by *A. tumefaciens*
799 C58 wild type were used for analysis. V1-3, V3-4, V5-7 and V6-8 represent different
800 primer pairs targeting different variable regions on 16S rRNA gene. (A) The OTU
801 counts of 16 rRNA gene amplicons after filtering non-bacterial OTUs. (ns, not
802 statistically significant; *, $p < 0.05$, student's t-test). The bar indicated mean of OTUs
803 ± SD. (B) Alpha rarefaction curves of the observed bacterial OTUs based on datasets
804 from amplicon sequencing run II. Sample size in X-axis indicates different sub-
805 sampling depth of each dataset.

806

807 **Figure 3. Gallobiome composition when using different primers amplified with**
808 **or without blockers.** (A) Different primer sets (V1-3, V3-4, V5-7 and V6-8**)** for
809 analysis of three crown gall samples (21W, 22W and 25W, see Table S6) induced by
810 *A. tumefaciens* C58 wild type were indicated. Top 10 observed families were listed.
811 "-": amplification without blockers; "+": amplification with blockers. Principle
812 coordinate analysis (PCoA) plots of the bacterial composition of the datasets were
813 generated based on the weighted Unifrac matrix, and color coded by (B) blocker

usage (*p*-value = 0.068, R^2 = 0.026, ADONIS), (C) different primer sets (*p*-value = 0.001, R^2 = 0.524, ADONIS) and (D) different crown gall samples (*p*-value = 0.001, R^2 = 0.238, ADONIS).

Figure 4. Principle coordinate analysis (PCoA) of bacterial composition in 53 crown galls induced by *A. tumefaciens* C58 WT and T6SS mutants.

The plots were drawn based on weighted Unifrac matrix of the bacterial communities. Crown galls induced by different C58 strains (WT, Δ*tssB,* Δ*tssL*) (A) or inoculated in different months (B) were labeled with different colors in each panel. The datasets were further split based on the month of inoculation, and the PCoA plots of gallobiomes from (C) July, (D) October and (E) November were indicated above. Statistical differences in clustering were evaluated via ADONIS permutation test, and the corresponding *p*-values and R^2 are indicated.

Figure 5. Alpha diversity and composition of crown galls generated in different months by *A. tumefaciens* C58 WT and T6SS mutants.

(A) Observed OTU, (B) Shannon index, (C) evenness, and (D) Faith's phylogenic diversity of each sample generated in different months was indicated. Lines and error bars indicate mean ± SD. Two-way ANOVA followed by Tukey's multiple comparisons test were performed, and the asterisks indicated the statistically significant difference between two strains (*p*-value < 0.05). (E) Bacterial composition of 53 crown galls. For each strain, the samples are grouped by the month of inoculation. Top-ten most abundant families were listed and colored differently, and the remaining ones are combined into "Others". (F) Relative abundance of *Rhizobiaceae* in galls inoculated in different months and strains. (G) Scatter plot of relative abundance of *A. tumefaciens* OTU in gallobiome - weight of the crown galls. A positive correlation between weight of crown gall and relative abundance of *A. tumefaciens* C58 was observed (Spearman r = 0.333, *p* = 0.01).

Figure 6. Analysis of composition of microbiomes (ANCOM) for gallobiomes in July.

The ANCOM volcano plots were drawn based on the centred-log-ratio-transformed abundance of (A) OTUs or bacterial families. The taxa that exhibit differential

847 abundance (DA) between gallobiomes induced by WT and T6SS mutants are
848 indicated by red arrows. The two DA OTUs belonging to *Sphingomonadaceae* were
849 named SphinOTU1 and SphinOTU2, respectively. The relative abundance of focal
850 taxa was shown in panels (B) and (C). Lines and error bars indicate mean ± SD.
851
852 **Fig. 7 Competition between *A. tumefaciens* C58 and *Sphingomonas* sp. R1 *in vitro***
853 **and on wounded site of tomato stems.**
854 Each of the three *A. tumefaciens* strains (i.e., C58 WT, Δ*tssL*, and Δ*tssB*) was
855 individually tested for competition against *Sphingomonas* sp. R1 isolated from
856 rhizosphere of tomato. (A) The *in vitro* competition results based on *A. tumefaciens*:
857 *Sphingomonas* sp. R1 at 1:1 and 10:1 ratio, and the survival of *Sphingomonas* sp. R1
858 was plotted; lines and error bars indicate mean ± SD. Based on ANOVA followed by
859 Tukey's multiple comparison test, C58 significantly reduced *Sphingomonas* sp. R1
860 CFUs when mixed in 10:1 ratio ($p = 0.0153$) but not in 1:1 ratio ($p = 0.2753$). (B) The
861 *A. tumefaciens* alone or co-infected with *Sphingomonas* sp. R1 at 1:1 ratio in soil
862 were recovered from the surface of wounded stem segments at 10 dpi, the CFU of *A.*
863 *tumefaciens* and *Sphingomonas* sp. R1 were plotted. T-test indicated the CFU
864 differences of *Sphingomonas* sp. R1 inoculation alone or co-infection with T6SS
865 mutants as compared to WT with indicated *p* values. ANOVA test indicated no
866 significant difference among means ($p = 0.0945$ and 0.0551 for *A. tumefaciens* and
867 *Sphingomonas* sp. R1 CFUs, respectively). (C) The colonies of *A. tumefaciens* strains
868 C58 WT, Δ*tssL*, and Δ*tssB* recovered from the surface of wounded stem segments
869 following the soil inoculation procedure were plotted. Different symbols indicated the
870 outcome from different batches of colonization assay. F-test indicated the variance of
871 Δ*tssL* and Δ*tssB* were significantly different when compared to C58 WT ($F =$
872 0.000467 and 8.04398E-05, respectively). Brown-Forsythe and Welch ANOVA test
873 indicated no significant difference among means ($p = 0.4847$). Line indicates median.
874

875 **Figure S1. DNA sequence alignment of 16S rRNA genes of selected bacterial**
876 **strains and tomato KnowYou 301 chloroplast and mitochondria.**
877 The 16S rRNA gene sequences of chloroplasts and mitochondria in *Solanum*
878 *lycopersicum* (tomato) cultivar Known-You 301 were obtained from this study. All of
879 the bacterial 16S rRNA gene sequences were accessed from Reference Sequence

880 (RefSeq) database in National Center of Biotechnology Information (NCBI). The
881 species, strain name, and accession number of 16S rRNA gene were listed at on the
882 left of each sequence. The alignment of sequences mentioned above were aligned in
883 MEGAX via ClustalW multiple alignment with gap opening penalty 15.00 and gap
884 extension penalty 6.66 (default). The levels of shaded blue color reflect the degree of
885 identity. The regions of each primer and blocker were underlined. The sequences
886 highlighted by red, black, yellow and green are the annealing region of primer sets for
887 V1-3, V3-4, V5-7 and V6-8 in 16S rRNA gene, respectively. And the gray framed
888 sequences in tomato chloroplast and mitochondrial 16S rRNA genes are the blockers
889 for cognate primers.

890

891 **Figure S2. Alpha rarefaction curves of the observed bacterial OTUs based on**
892 **amplicon sequencing of 53 gall samples in sequencing run III.**
893 The rarefaction curves were plotted after clustering DADA2-output ASVs into 99%
894 OTUs. Sample size in X-axis indicates different sub-sampling depth of each dataset;
895 Species in Y-axis indicates the number of observed OTUs under certain sub-sampling
896 depth. Label of each curves indicates the sample ID in metadata.

897

898 **Figure S3. Competition of *A. tumefaciens* and *Sphingomonas* sp. R1 in tomato**
899 **gall on stem at 28 dpi.**
900 Each of the three *A. tumefaciens* strains (i.e., C58 WT, Δ*tssL*, and Δ*tssB*) and R1 were
901 mixed at 1:1 ratio then inoculated on wounded tomato stem. The galls were harvested
902 and homogenized for plating at 28 dpi. *A. tumefaciens* C58 strains and *Sphingomonas*
903 sp. R1 were recover on 523 medium plates containing proper antibiotics. R1 could
904 only be recovered from galls in batch 3. The *p*-value of ANOVA against CFU
905 numbers of C58 for each batch is 0.786, 0.0023 and 0.230; the *p*-value of ANOVA
906 against CFU numbers of R1 was 0.6413. The significance of CFU numbers of C58 in
907 second batch is due to the low CFU counts of Δ*tssL* single inoculation group, which
908 could not be replicated in other two batches.

909

910

911

912

Table 1. Incidences of crown gall disease on wounded tomato stems by soil inoculation

Batch	Date of inoculation	Disease incidence (diseased/total inoculated seedlings)		
		C58 WT[a]	Δ*tssL*[b]	Δ*tssB*[b]
1	2018/11/15	0.86 (12/14)	0.86 (12/14)	N.D.*
2	2018/12/20	0.30 (6/20)	0.45 (9/20)	N.D.
3	2019/06/10	0.10 (2/20)	0.05 (1/20)	0.05 (1/20)
4	2019/07/04	0.35 (7/20)	0.35 (7/20)	0.26 (5/19)
5	2019/07/22	0.30 (6/20)	0.00 (0/20)	0.10 (2/20)
6	2019/07/29	0.27 (4/15)	0.27 (4/15)	0.14 (2/14)
7	2019/10/05	0.35 (7/20)	0.25 (5/20)	0.30 (6/20)
8	2019/10/30	0.50 (8/16)	0.25 (4/16)	0.38 (6/16)
9	2010/11/11	0.94 (15/16)	0.56 (9/16)	0.50 (8/16)

[a, b]: Two-way ANOVA followed by Tukey's multiple comparisons test on disease incidences of different strains indicated the disease incidence of Δ*tssL* and Δ*tssB* was significantly lower than *A. tumefaciens* C58 WT (*p*-value are 0.0225 and 0.0227 respectively). *: Not Determined.

Table 2. Sum of read counts in six tumor samples before and after filtering non-bacterial reads from amplicon sequencing run I for protocol test

16S rRNA regions	Before filtering	Bacterial reads	Percentage of non-bacterial DNA
V3-4	140,830	1,230	99.1%
V5-7	601,299	38,320	93.6%

Table 3 The read count before and after filtering non-bacterial ASVs from the three crown gall DNA samples (named as W21, W22, and W25) induced by *A. tumefaciens* C58 wild type

Sample-id	Dataset-id	Read before filtering	Reads after filtering chloroplast and mitochondrial DNA	Percentage of non-host reads
1115-21W	T21-v1-3-B	176,544	9,914	5.6%
1115-22W	T22-v1-3-B	183,475	5,608	3.1%
1115-25W	T25-v1-3-B	152,387	2,404	1.6%
1115-21W	T21-v1-3-A	185,107	853	0.5%
1115-22W	T22-v1-3-A	247,240	379	0.2%
1115-25W	T25-v1-3-A	178,980	220	0.1%
1115-21W	T21-v3-4-B	239,243	38,462	16.1%
1115-22W	T22-v3-4-B	246,063	19,218	7.8%
1115-25W	T25-v3-4-B	209,991	11,185	5.3%
1115-21W	T21-v3-4-A	200,185	979	0.5%
1115-22W	T22-v3-4-A	205,966	796	0.4%
1115-25W	T25-v3-4-A	193,350	426	0.2%
1115-21W	T21-v5-7-B	129,422	53,715	41.5%
1115-22W	T22-v5-7-B	140,012	29,078	20.8%
1115-25W	T25-v5-7-B	135,692	18,052	13.3%
1115-21W	T21-v5-7-A	150,015	2,792	1.9%
1115-22W	T22-v5-7-A	139,974	1,507	1.1%
1115-25W	T25-v5-7-A	133,035	786	0.6%
1115-21W	T21-v6-8-B	92,167	3,691	4.0%
1115-22W	T22-v6-8-B	92,053	3,197	3.5%
1115-25W	T25-v6-8-B	82,361	2,077	2.5%
1115-21W	T21-v6-8-A	121,145	1,604	1.3%
1115-22W	T22-v6-8-A	138,186	1,273	0.9%
1115-25W	T25-v6-8-A	121,820	708	0.6%
	NC-v3-4-B	1,012	979	96.7%

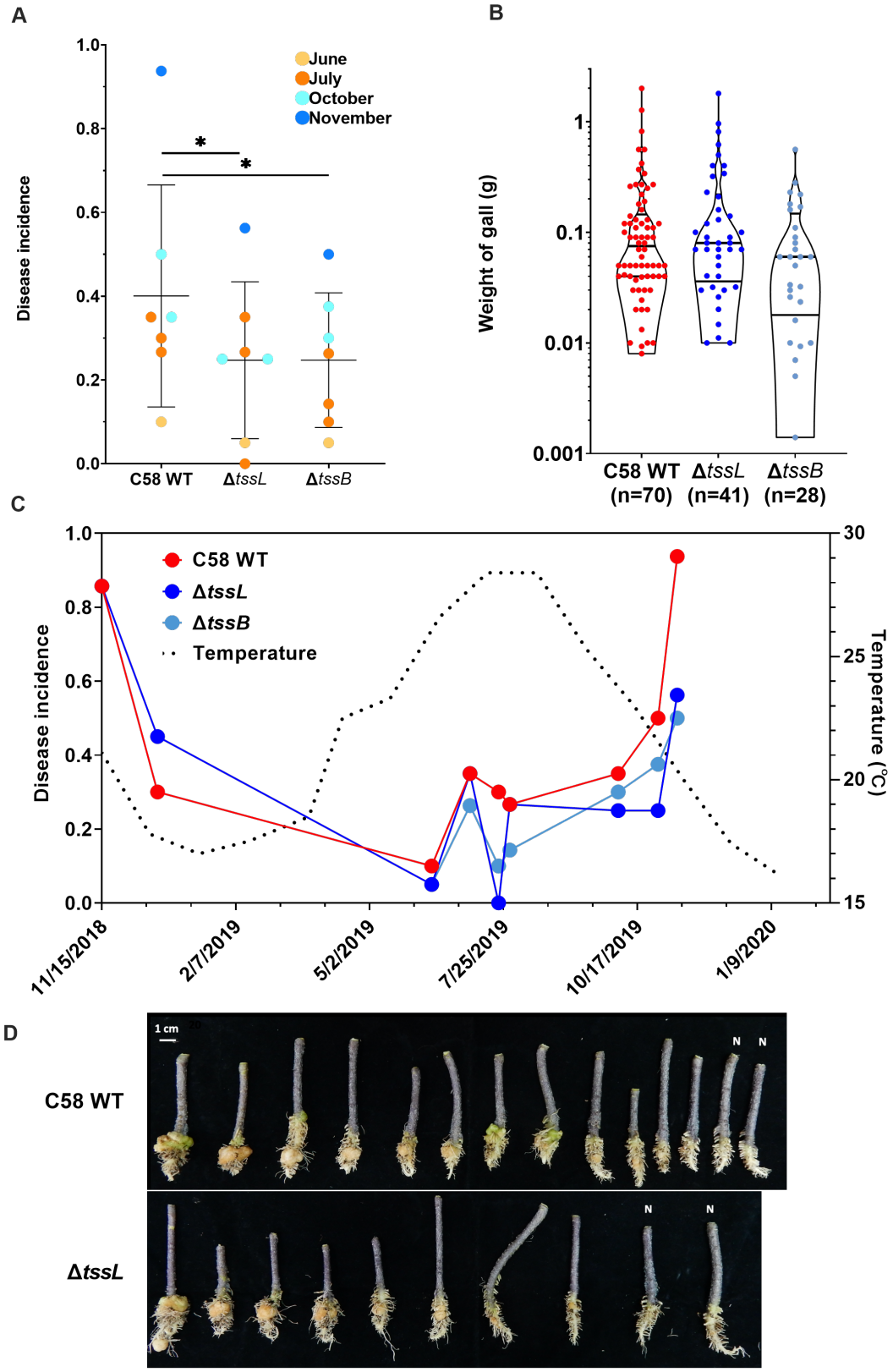

Figure 1. Tumorigenesis assay of *A. tumefaciens* C58 and its T6SS-deficienct mutants.

For each experiment, 14-20 wounded tomato seedlings were grown in soil containing

one of the strains tested (i.e., C58 WT, Δ*tssL*, and Δ*tssB*) and collected at 60 days post inoculation (dpi). (A) Disease incidence plotted by strain and color-coded according to the month of inoculation (light yellow, June; orange, July; light blue, October; dark blue, November). Lines and error bars indicate mean ± SD. Statistical significance was tested using two-way ANOVA followed by Tukey's multiple comparisons; p = 0.025 and 0.027 when comparing the wild type to Δ*tssL* and Δ*tssB*, respectively. (B) Weight distribution of the galls collected. No significant difference among the three strains (p = 0.15, Kruskai-Wallis test). (C) Correlation plot of disease incidence and temperature of daily average. (D) Crown galls generated through soil inoculation, example from inoculation on 11/15/2018. N indicated no gall formation in some of inoculated plants.

17

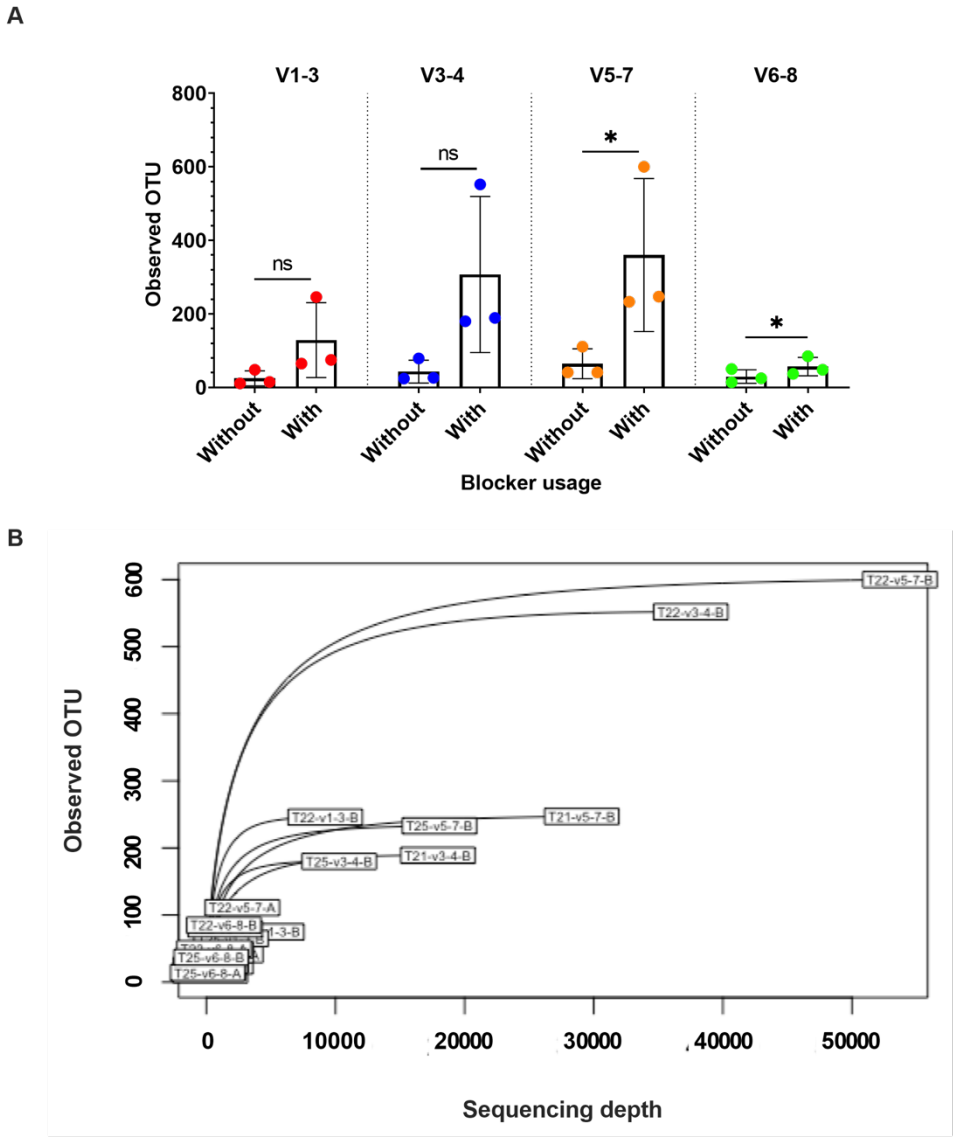

18

19 **Figure 2. Optimizing 16S rRNA gene amplification by using PCR blockers.**
20 Three crown gall samples (named as 21W, 22W and 25W) induced by *A. tumefaciens*
21 C58 wild type were used for analysis. V1-3, V3-4, V5-7 and V6-8 represent different
22 primer pairs targeting different variable regions on 16S rRNA gene. (A) The OTU
23 counts of 16 rRNA gene amplicons after filtering non-bacterial OTUs. (ns, not
24 statistically significant; *, $p < 0.05$, student's t-test). The bar indicated mean of OTUs
25 ± SD. (B) Alpha rarefaction curves of the observed bacterial OTUs based on datasets
26 from amplicon sequencing run II. Sample size in X-axis indicates different sub-
27 sampling depth of each dataset.

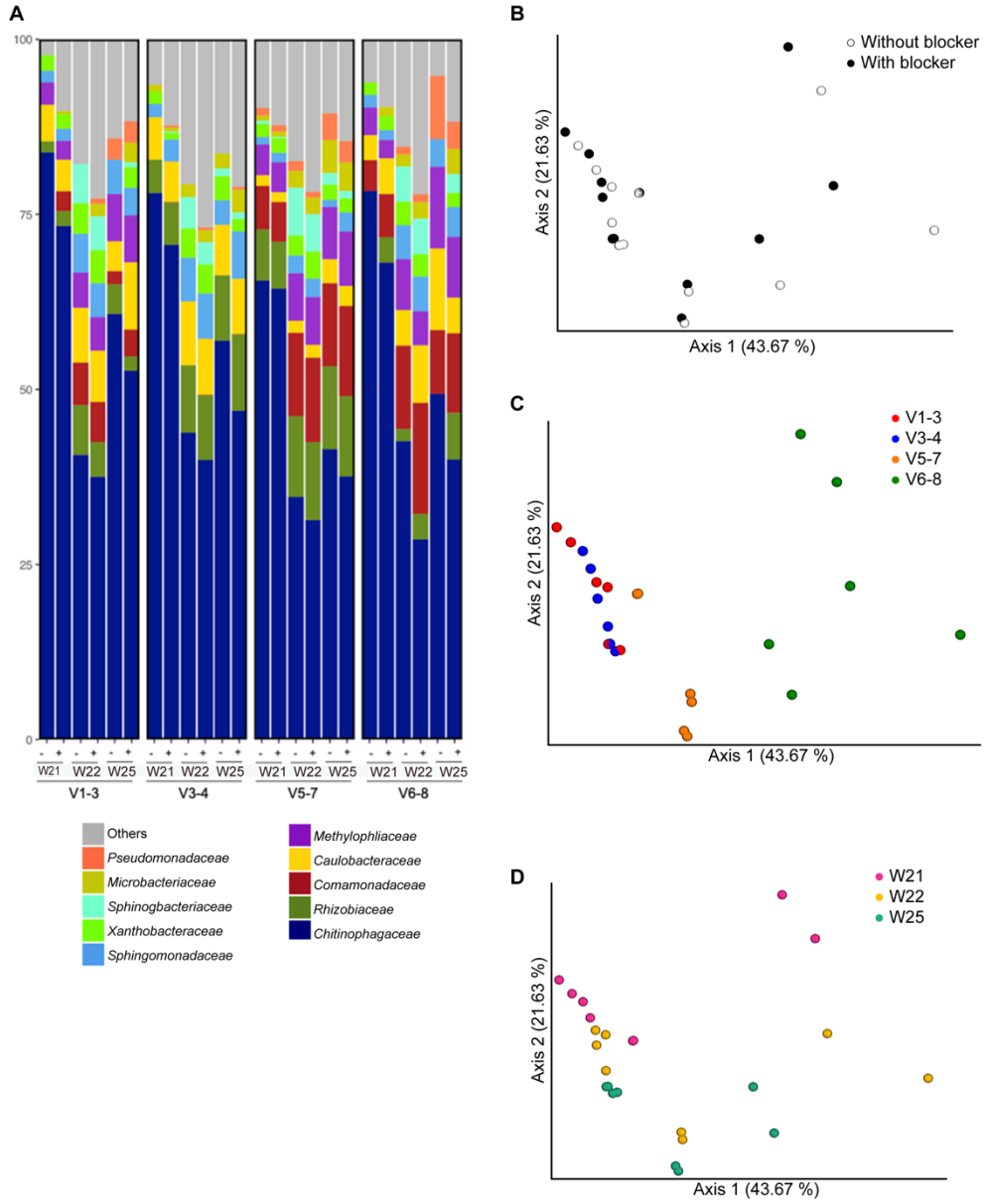

Figure 3. Gallobiome composition when using different primers amplified with or without blockers. (A) Different primer sets (V1-3, V3-4, V5-7 and V6-8**)** for analysis of three crown gall samples (21W, 22W and 25W, see Table S6) induced by *A. tumefaciens* C58 wild type were indicated. Top 10 observed families were listed. "-": amplification without blockers; "+": amplification with blockers. Principle coordinate analysis (PCoA) plots of the bacterial composition of the datasets were generated based on the weighted Unifrac matrix, and color coded by (B) blocker usage (p-value = 0.068, R^2 = 0.026, ADONIS), (C) different primer sets (p-value = 0.001, R^2 = 0.524, ADONIS) and (D) different crown gall samples (p-value = 0.001, R^2 = 0.238, ADONIS).

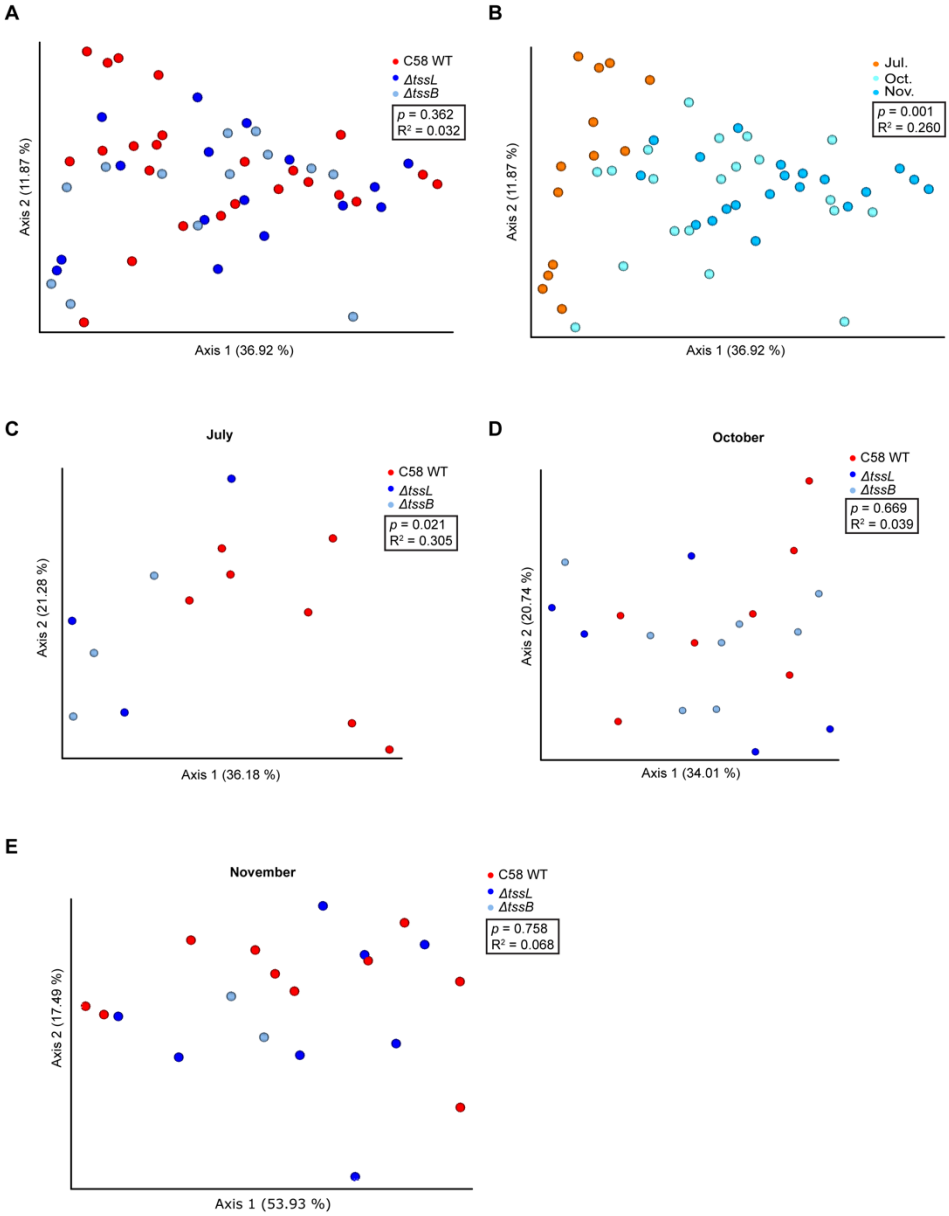

Figure 4. Principle coordinate analysis (PCoA) of bacterial composition in 53 crown galls induced by *A. tumefaciens* C58 WT and T6SS mutants.

The plots were drawn based on weighted Unifrac matrix of the bacterial communities. Crown galls induced by different C58 strains (WT, Δ*tssB,* Δ*tssL*) (A) or inoculated in different months (B) were labeled with different colors in each panel. The datasets were further split based on the month of inoculation, and the PCoA plots of gallobiomes from (C) July, (D) October and (E) November were indicated above. Statistical differences in clustering were evaluated via ADONIS permutation test, and the corresponding *p*-values and R^2 are indicated.

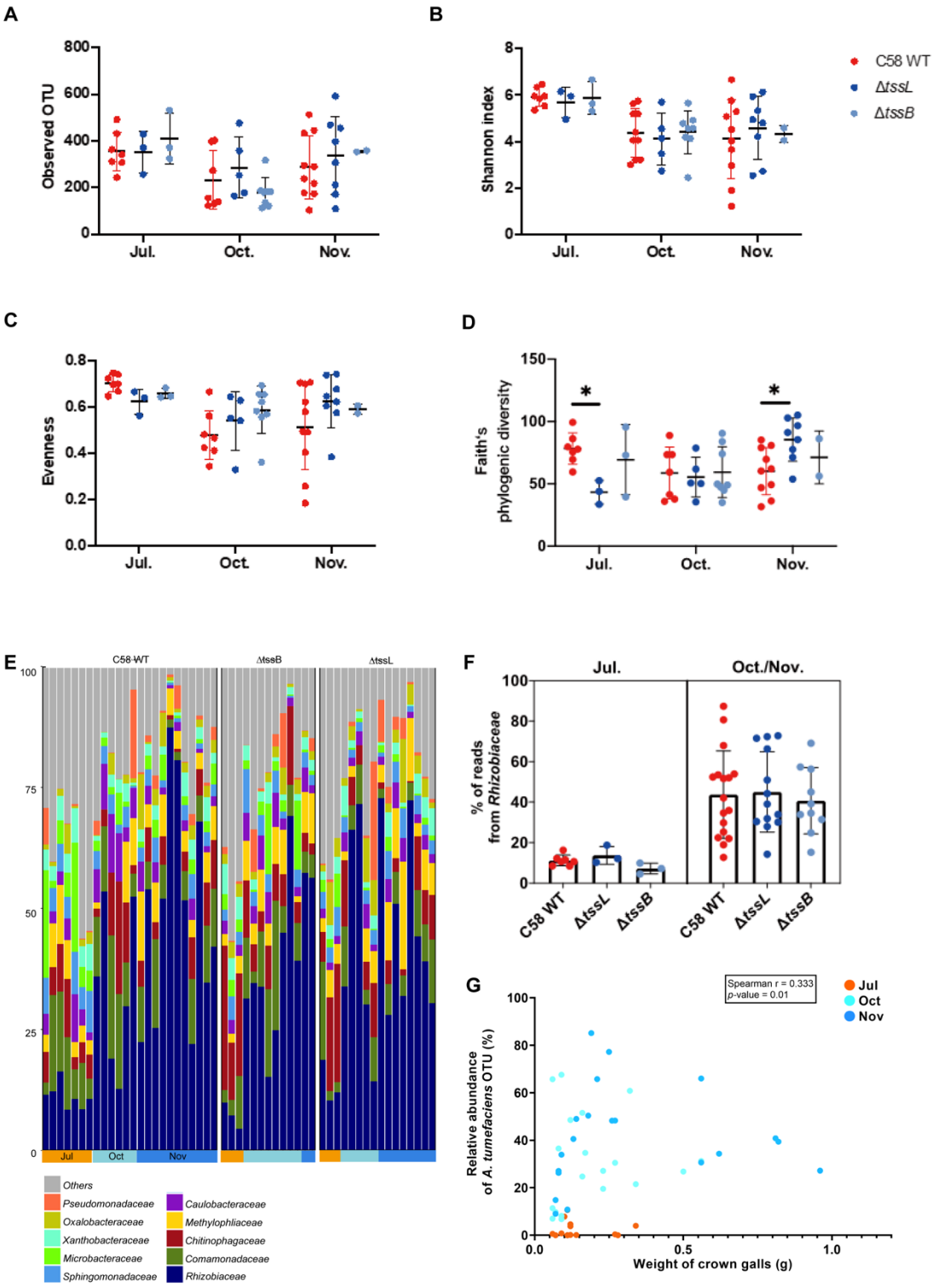

Figure 5. Alpha diversity and composition of crown galls generated in different months by *A. tumefaciens* C58 WT and T6SS mutants.

(A) Observed OTU, (B) Shannon index, (C) evenness, and (D) Faith's phylogenic diversity of each sample generated in different months was indicated. Lines and error bars indicate mean ± SD. Two-way ANOVA followed by Tukey's multiple comparisons test were performed, and the asterisks indicated the statistically

significant difference between two strains (p-value < 0.05). (E) Bacterial composition of 53 crown galls. For each strain, the samples are grouped by the month of inoculation. Top-ten most abundant families were listed and colored differently, and the remaining ones are combined into "Others". (F) Relative abundance of *Rhizobiaceae* in galls inoculated in different months and strains. (G) Scatter plot of relative abundance of *A. tumefaciens* OTU in gallobiome - weight of the crown galls. A positive correlation between weight of crown gall and relative abundance of *A. tumefaciens* C58 was observed (Spearman r = 0.333, p = 0.01).

66

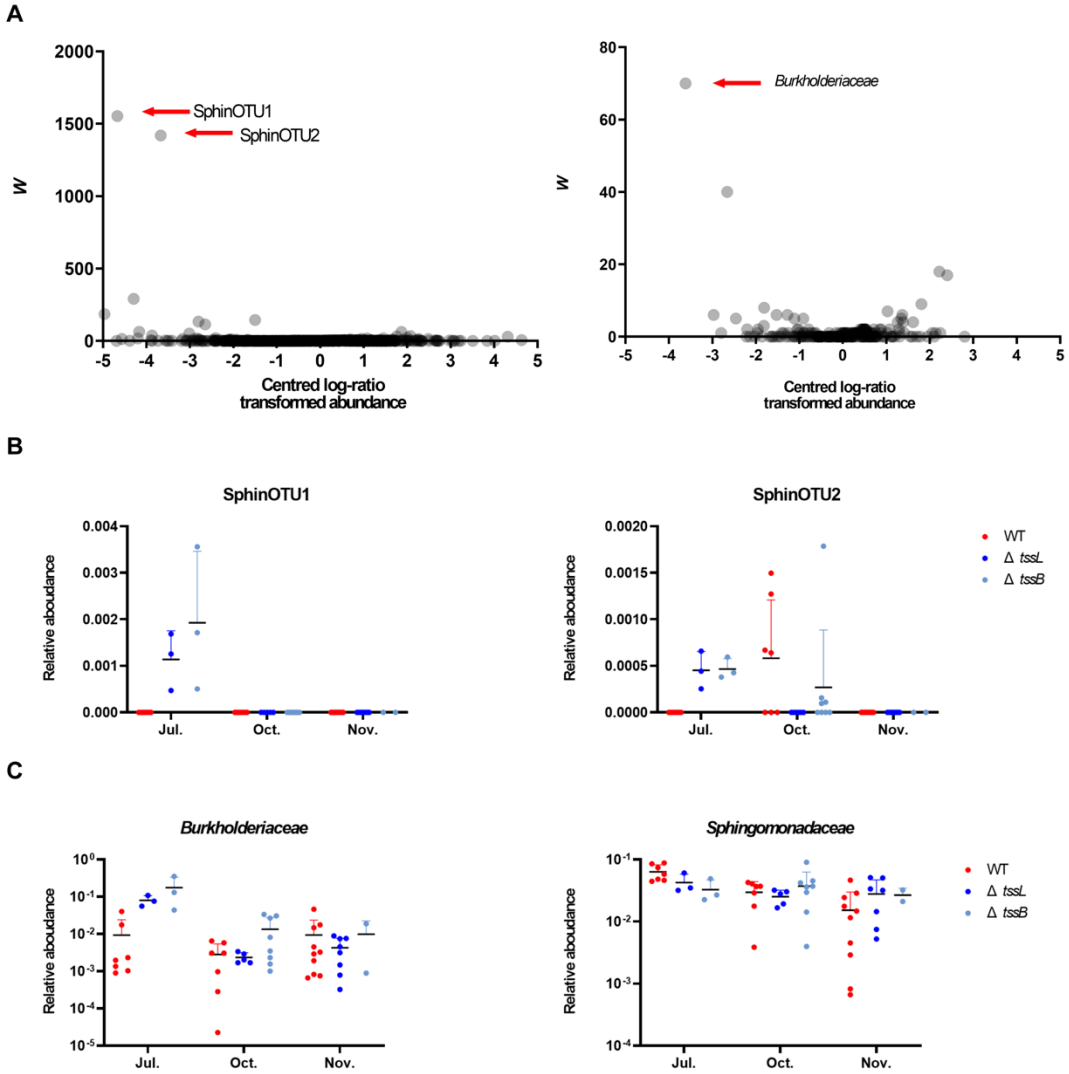

67

68 **Figure 6. Analysis of composition of microbiomes (ANCOM) for gallobiomes in**
69 **July.**

70 The ANCOM volcano plots were drawn based on the centred-log-ratio-transformed
71 abundance of (A) OTUs or bacterial families. The taxa that exhibit differential
72 abundance (DA) between gallobiomes induced by WT and T6SS mutants are
73 indicated by red arrows. The two DA OTUs belonging to *Sphingomonadaceae* were
74 named SphinOTU1 and SphinOTU2, respectively. The relative abundance of focal
75 taxa was shown in panels (B) and (C). Lines and error bars indicate mean ± SD.

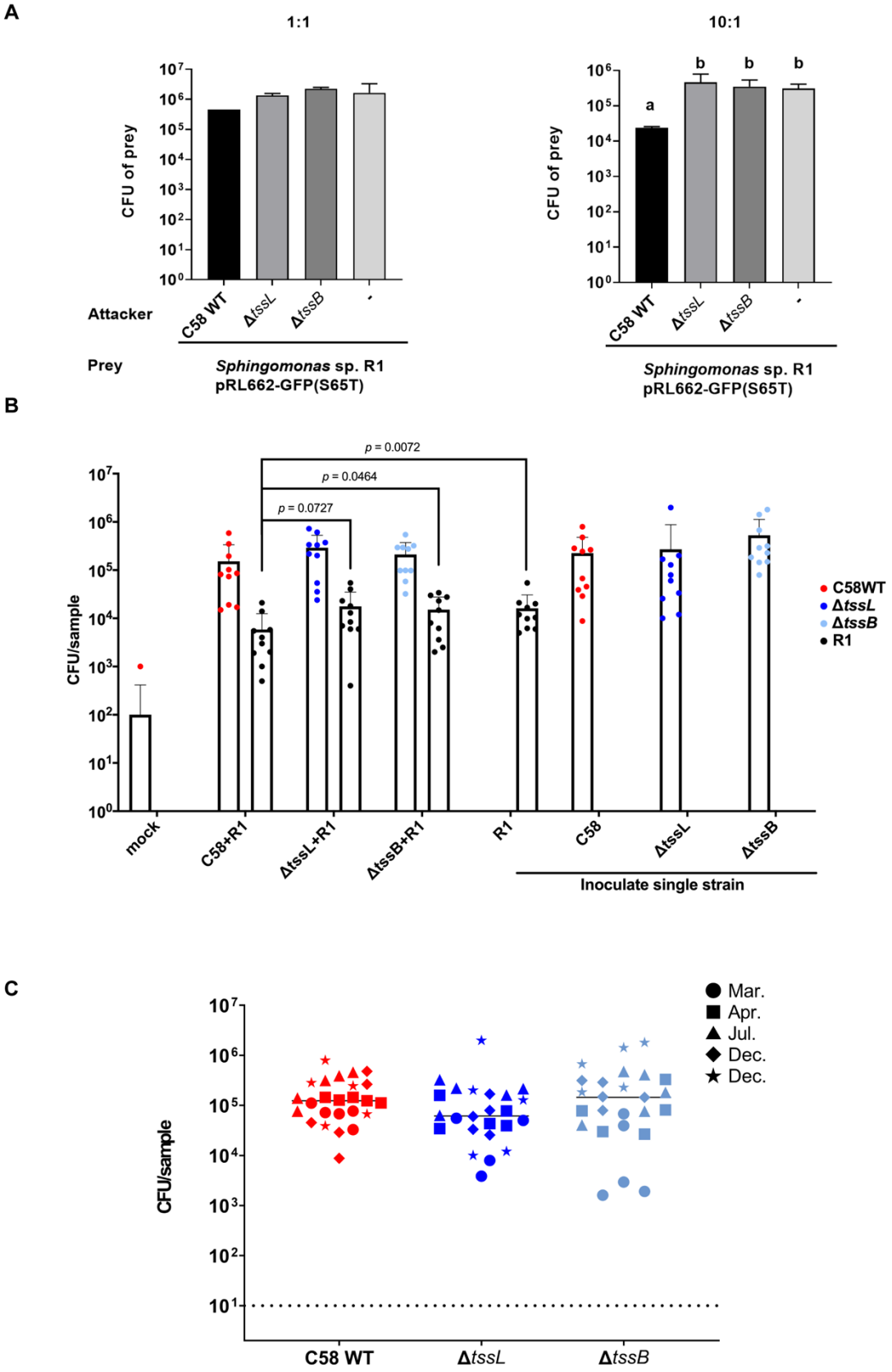

Fig. 7 Competition between *A. tumefaciens* C58 and *Sphingomonas* sp. R1 *in vitro* and on wounded site of tomato stems.

Each of the three *A. tumefaciens* strains (i.e., C58 WT, Δ*tssL*, and Δ*tssB*) was individually tested for competition against *Sphingomonas* sp. R1 isolated from rhizosphere of tomato. (A) The *in vitro* competition results based on *A. tumefaciens*: *Sphingomonas* sp. R1 at 1:1 and 10:1 ratio, and the survival of *Sphingomonas* sp. R1 was plotted; lines and error bars indicate mean ± SD. Based on ANOVA followed by Tukey's multiple comparison test, C58 significantly reduced *Sphingomonas* sp. R1 CFUs when mixed in 10:1 ratio ($p = 0.0153$) but not in 1:1 ratio ($p = 0.2753$). (B) The *A. tumefaciens* alone or co-infected with *Sphingomonas* sp. R1 at 1:1 ratio in soil were recovered from the surface of wounded stem segments at 10 dpi, the CFU of *A. tumefaciens* and *Sphingomonas* sp. R1 were plotted. T-test indicated the CFU differences of *Sphingomonas* sp. R1 inoculation alone or co-infection with T6SS mutants as compared to WT with indicated *p* values. ANOVA test indicated no significant difference among means ($p = 0.0945$ and 0.0551 for *A. tumefaciens* and *Sphingomonas* sp. R1 CFUs, respectively). (C) The colonies of *A. tumefaciens* strains C58 WT, Δ*tssL*, and Δ*tssB* recovered from the surface of wounded stem segments following the soil inoculation procedure were plotted. Different symbols indicated the outcome from different batches of colonization assay. F-test indicated the variance of Δ*tssL* and Δ*tssB* were significantly different when compared to C58 WT ($F = 0.000467$ and 8.04398E-05, respectively). Brown-Forsythe and Welch ANOVA test indicated no significant difference among means ($p = 0.4847$). Line indicates median.

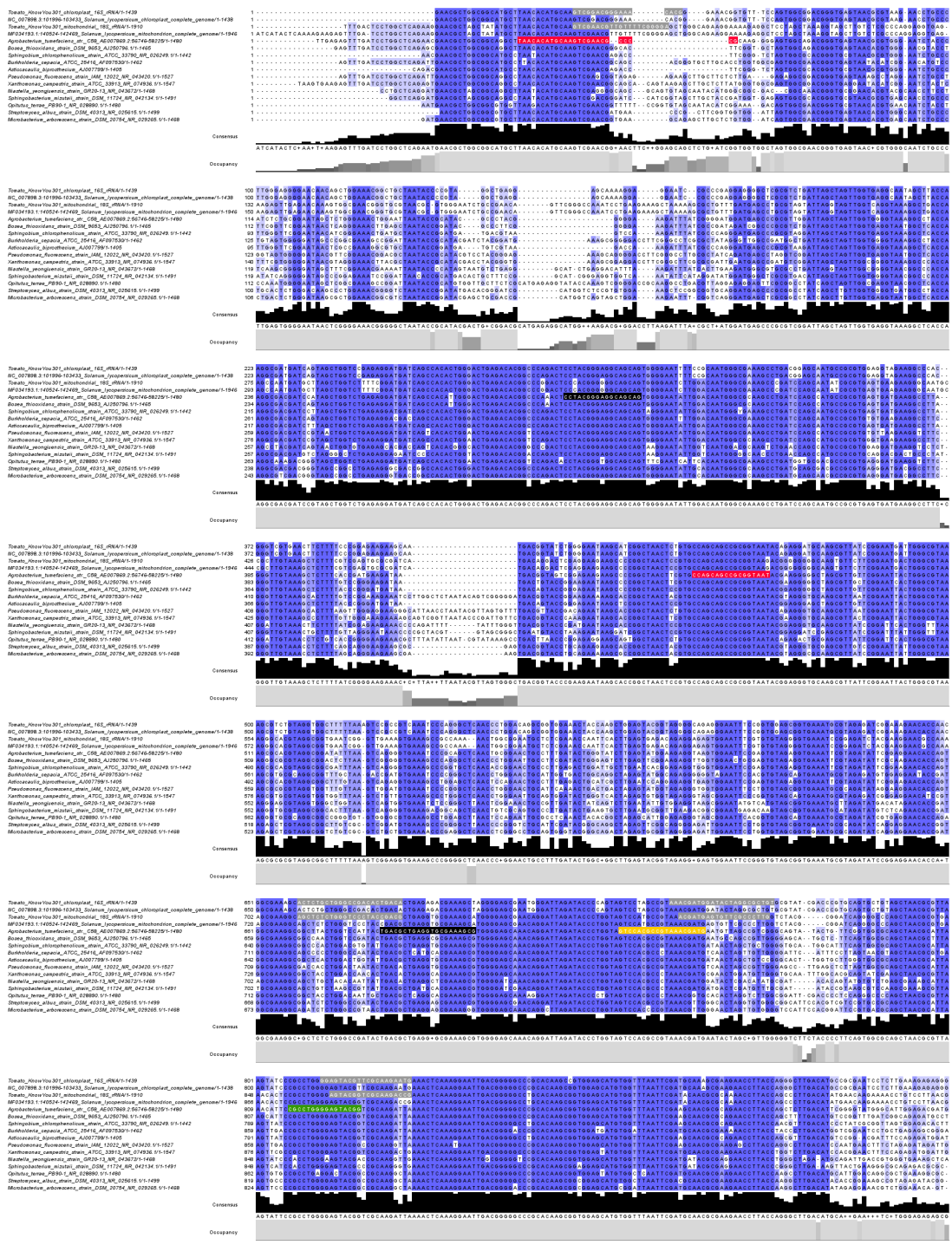

99

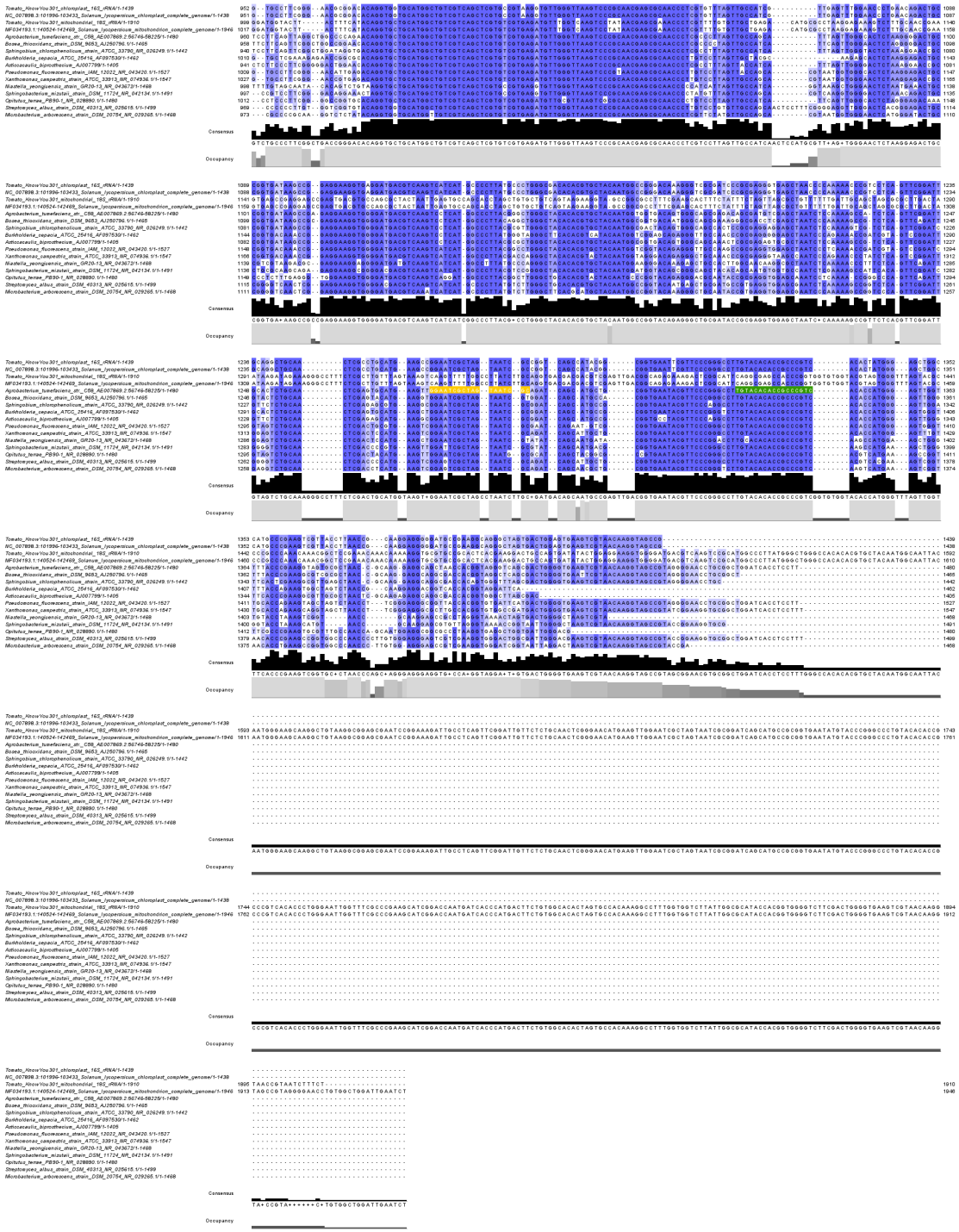

Figure S1. DNA sequence alignment of 16S rRNA genes of selected bacterial strains and tomato KnowYou 301 chloroplast and mitochondria.

The 16S rRNA gene sequences of chloroplasts and mitochondria in *Solanum lycopersicum* (tomato) cultivar Known-You 301 were obtained from this study. All of the bacterial 16S rRNA gene sequences were accessed from Reference Sequence (RefSeq) database in National Center of Biotechnology Information (NCBI). The species, strain name, and accession number of 16S rRNA gene were listed at on the

left of each sequence. The alignment of sequences mentioned above were aligned in MEGAX via ClustalW multiple alignment with gap opening penalty 15.00 and gap extension penalty 6.66 (default). The levels of shaded blue color reflect the degree of identity. The regions of each primer and blocker were underlined. The sequences highlighted by red, black, yellow and green are the annealing region of primer sets for V1-3, V3-4, V5-7 and V6-8 in 16S rRNA gene, respectively. And the gray framed sequences in tomato chloroplast and mitochondrial 16S rRNA genes are the blockers for cognate primers.

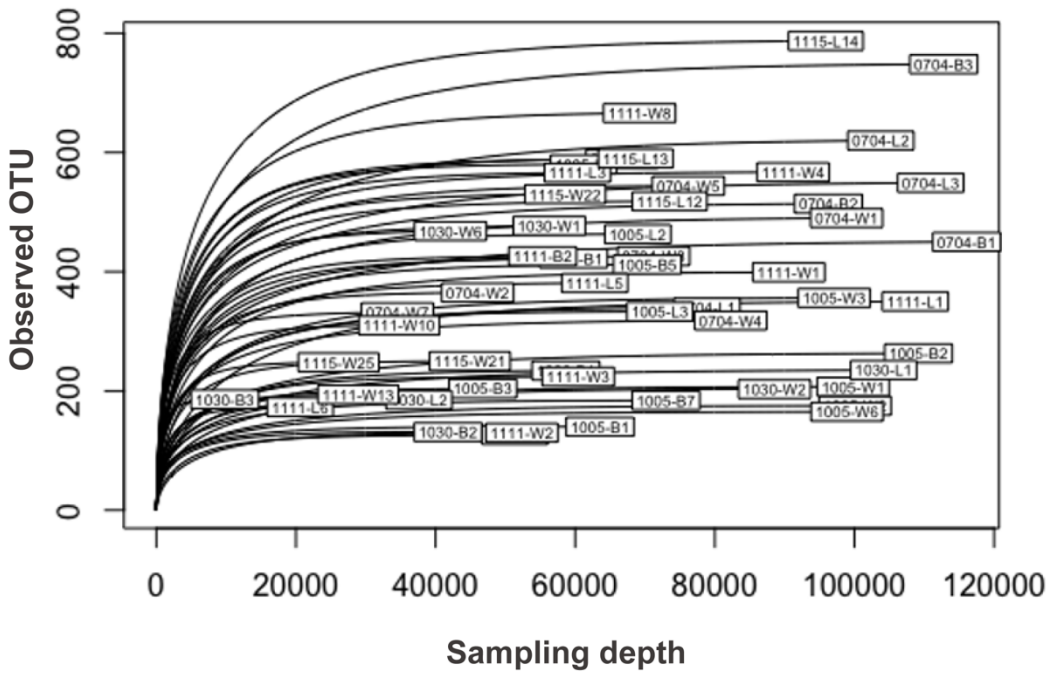

Figure S2. Alpha rarefaction curves of the observed bacterial OTUs based on amplicon sequencing of 53 gall samples in sequencing run III.

The rarefaction curves were plotted after clustering DADA2-output ASVs into 99% OTUs. Sample size in X-axis indicates different sub-sampling depth of each dataset; Species in Y-axis indicates the number of observed OTUs under certain sub-sampling depth. Label of each curves indicates the sample ID in metadata.

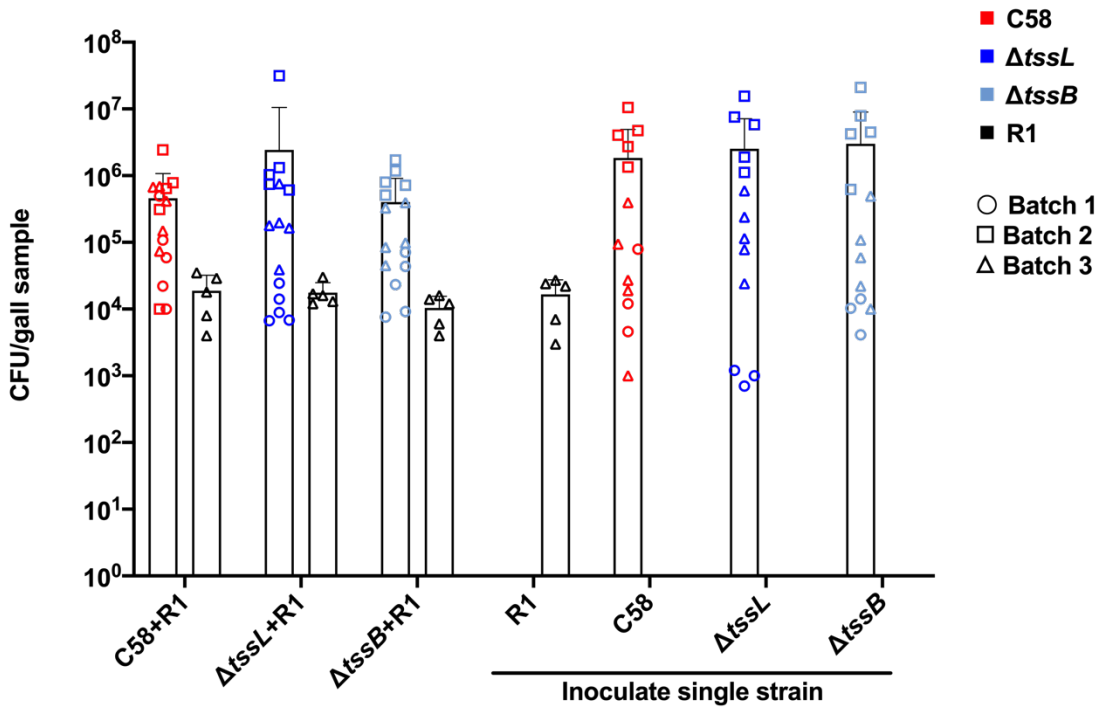

Figure S3. Competition of *A. tumefaciens* and *Sphingomonas* sp. R1 in tomato gall on stem at 28 dpi.

Each of the three *A. tumefaciens* strains (i.e., C58 WT, Δ*tssL*, and Δ*tssB*) and R1 were mixed at 1:1 ratio then inoculated on wounded tomato stem. The galls were harvested and homogenized for plating at 28 dpi. *A. tumefaciens* C58 strains and *Sphingomonas* sp. R1 were recover on 523 medium plates containing proper antibiotics. R1 could only be recovered from galls in batch 3. The *p*-value of ANOVA against CFU numbers of C58 for each batch is 0.786, 0.0023 and 0.230; the *p*-value of ANOVA against CFU numbers of R1 was 0.6413. The significance of CFU numbers of C58 in second batch is due to the low CFU counts of *ΔtssL* single inoculation group, which could not be replicated in other two batches.

Table S1. 16S rRNA gene primer sets used in this study

Targeted Region	Name	Sequence (5'-3')	Size of bacterial amplicons (bp)	Size of tomato amplicons (bp)*
Round I				
V3-V4	341F 785R	CCTACGGGNGGCWGCAG GACTACHVGGGTATCTAATC C	444	396 (cp); 395 (mt)
V5-V7	799F 1193R	AACMGGATTAGATACCCKG ACGTCATCCCCACCTTCC	394	376(cp); 742(mt)
Round II				
V1-V3	68F 518R	TNANACATGCAAGTCGRRCG WTTACCGCGGCTGCTGG	425	440 (cp); 474(mt)
V3-V4	**341F** **688R**	CCTACGGGNGGCWGCAG CGCTTTCGHDCCTCAGYGTC A	429 405	408 (cp); 391(mt)
V5-V7	**819F** **1276R**	GTCCACVCCSTAAACGWTG RCGATTACTAGCGAHTCC	553	551 (cp); 915(mt)
V6-V8	**895F** **1391R**	CRCCTGGGGAGTRCRG GACGGGCGGTGTGTRCA	530	527 (cp); 894 (mt)

*cp, chloroplast; mt, mitochondrion

Table S2. Corresponding blockers (3' modified oligonucleotides with C3 spacer)

Targeted Region	Name*	Sequence	Tm (℃)
V1	68f_blocker_mt	GTCGAACGTTGTTTTCGGGGAG	62
V1	68f_blocker_cp	GTCGGACGGGAAACACG	61
V4	688ra_blocker_mt	CGTCGGTAGGGACCCAGAGAGCT	69
V4	688ra_blocker_cp	TGTCAGTGTCGGCCCAGCAGAGT	69
V5	819f_blocker_mt	ACGATGAGTGTTCGCCCTTG	61
V5	819f_blocker_cp	AAACGATGGATACTAGGTGCTGT	60
V6	895f_blocker_mt	AGTACGGTCGCAAGACCG	61
V6	895f_blocker_cp	GGAGTACGTTCGCAAGAATG	60

* cp, chloroplast; mt, mitochondrion

Table S3. Bacteria strains and plasmid in this study

Strain/plasmid	Characteristics	EML No.	Reference/ Source
***Escherichia coli* DH10B**	Host for DNA cloning	455	Invitrogen
***Agrobacterium tumefaciens* C58**	Wild-type, virulent strain containing nonpaline-type Ti-plasimid, pTiC58	530	Eugene Nester [1]
	Δ*tssL*, deletion mutant of *tssL* gene (Atu4333)	1073	[2]
	Δ*tssB*, deletion mutant of *tssB* gene (Atu4342)	1109	[2]
	Gm^R-GFP knocked-in chromosome	4094	This study
	Δ*tssL*, Gm^R-GFP knocked-in chromosome	4097	This study
	Δ*tssB*, Gm^R-GFP knocked-in chromosome	4100	This study
***Sphingomonas sp.* R1**	Wild type, isolated from tomato rhizosphere	4107	This study
pJQ-COM	Gm^R, for generating DNA knock-in adjacent to gene *ActC* in C58	2236	[3]
pJQ-com-Gm^r GFP	Gm^R, for generate Gm^R and GFP knocked-in C58	4091	This study
pRL662::GFP (S65T)	Gm^R, constitutively expressing GFP (S56T)	3375	This study
pBBR1MCS2-mCherry	Km^R, constitutively expressing mCherry	3022	Stanton B. Gelvin

Table S4. Primers for plasmid construction

Name	Sequence	Reference
BclI-GFP-GmR-F-25	AAAAATGATCAGTGAGCGCGCGTAATACGACTCAC	This study
BclI-GFP-GmR-R-25	AAAAATGATCAGGGTACCGAGCTCGAATTGACATAAG	This study
3'sacB-5'GmR pJQ200 F	TGCGCCAAGCTTCCTGCTGAACATC	This study
3'sacB-5'GmR pJQ200 R	TTGAGCAGCCGCGTAGTGAGATCTA	This study

Table S5. Condition of 16S rRNA gene amplification

1st PCR Amplification v1-3									2nd Library Amplification				
Recipe A		**Program**			**Recipe B**		**Program**			**Recipe**		**Program**	
input 25 ng	6.5	95℃	5 min	1 cycle	input 25 ng	6.5	95℃	5 min	1 cycle	1st purified PCR products	20	98℃	2 min	1 cycle
H2O		98℃	30 sec		H2O		98℃	30 sec		H2O		98℃	**30** sec	
2X **Kapa HiFi PCR mix**	12.5	**55℃**	30 sec	12cycle	2X **Kapa HiFi PCR mix**	12.5	**55℃**	30 sec	15cycle	2X **Kapa HiFi PCR mix**	25	60℃	30 sec	**5** cycle
68f primer 10uM (final 0.2uM)	0.5	72℃	60 sec		68f primer 10uM (final 0.2uM)	0.5	72℃	60 sec		Truseq-HT-D5xx_F (10uM)	2.5	72℃	60 sec	
518r primer 10uM (final 0.2uM)	0.5	72℃	5 min	1 cycle	518r primer 10uM (final 0.2uM	0.5	72℃	5 min	1 cycle	Truseq-HT-D7xx_R (10uM)	2.5	72℃	5 min	1 cycle
H2O	5	4℃	∞	1 cycle	68f_blocking_mito 20uM	2.5	4℃	∞	1 cycle	Total	50	10℃	∞	1 cycle
					518r_blocking_chloro_20uM	2.5								
Total	25				Total	25				25uL/tube				
Beads purificatin, 1:1					Beads purificatin, 1:1					Beads purificatin, 1:1				

1st PCR Amplification v3-4									2nd Library Amplification				
Recipe A		**Program**			**Recipe B**		**Program**			**Recipe**		**Program**	
input 25 ng	6.5	95℃	5 min	1 cycle	input 25 ng	6.5	95℃	5 min	1 cycle	1st purified PCR products	20	98℃	2 min	1 cycle
H2O		98℃	30 sec		H2O		98℃	30 sec		H2O		98℃	**30** sec	**5** cycle **(A)**
2X **Kapa HiFi PCR mix**	12.5	**56℃**	30 sec	18cycle	2X **Kapa HiFi PCR mix**	12.5	**56℃**	30 sec	18 cycle	2X **Kapa HiFi PCR mix**	25	60℃	30 sec	**10** cycle **(B)**
341f primer 10uM (final 0.2uM)	0.5	72℃	60 sec		341f primer 10uM (final 0.2uM	0.5	72℃	60 sec		Truseq-HT-D5xx_F (10uM)	2.5	72℃	60 sec	
688ar primer 10uM (final 0.2uM	0.5	72℃	5 min	1 cycle	688ar primer 10uM (final 0.2uf	0.5	72℃	5 min	1 cycle	Truseq-HT-D7xx_R (10uM)	2.5	72℃	5 min	1 cycle
H2O	5	4℃	∞	1 cycle	688ar_blocking_mito 20uM	2.5	4℃	∞	1 cycle	Total	50	10℃	∞	1 cycle
					688ar_blocking_chloro_20uM	2.5								
Total	25				Total	25				25uL/tube				
Beads purificatin, 1:1					Beads purificatin, 1:1					Beads purificatin, 1:1				

1st PCR Amplification v5-7									2nd Library Amplification				
Recipe A		**Program**			**Recipe B**		**Program**			**Recipe**		**Program**	
input 25 ng	6.5	95℃	5 min	1 cycle	input 25 ng	6.5	95℃	5 min	1 cycle	1st purified PCR products	20	98℃	2 min	1 cycle
H2O		98℃	30 sec		H2O		98℃	30 sec		H2O		98℃	**30** sec	
2X **Kapa HiFi PCR mix**	12.5	**56℃**	30 sec	20cycle	2X **Kapa HiFi PCR mix**	12.5	**56℃**	30 sec	24cycle	2X **Kapa HiFi PCR mix**	25	60℃	30 sec	**5** cycle
819f primer 10uM (final 0.2uM)	0.5	72℃	60 sec		819f primer 10uM (final 0.2uM	0.5	72℃	60 sec		Truseq-HT-D5xx_F (10uM)	2.5	72℃	60 sec	
1276r primer 10uM (final 0.2uM	0.5	72℃	5 min	1 cycle	1276r primer 10uM (final 0.2uf	0.5	72℃	5 min	1 cycle	Truseq-HT-D7xx_R (10uM)	2.5	72℃	5 min	1 cycle
H2O	5	4℃	∞	1 cycle	819f_blocking_mito 20uM	2.5	4℃	∞	1 cycle	Total	50	10℃	forever	1 cycle
					819f_blocking_chloro_20uM	2.5								
Total	25				Total	25				25uL/tube				
Beads purificatin, 1:1					Beads purificatin, 1:1					Beads purificatin, 1:1				

1st PCR Amplification v6-8									2nd Library Amplification				
Recipe A		**Program**			**Recipe B**		**Program**			**Recipe**		**Program**	
input 25 ng	6.5	95℃	5 min	1 cycle	input 25 ng	6.5	95℃	5 min	1 cycle	1st purified PCR products	20	98℃	2 min	1 cycle
H2O		98℃	30 sec		H2O		98℃	30 sec		H2O		98℃	**30** sec	
2X **Kapa HiFi PCR mix**	12.5	**50℃**	30 sec	11cycle	2X **Kapa HiFi PCR mix**	12.5	**50℃**	30 sec	12cycle	2X **Kapa HiFi PCR mix**	25	60℃	30 sec	**5** cycle
895f primer 10uM (final 0.2uM)	0.5	72℃	60 sec		895f primer 10uM (final 0.2uM	0.5	72℃	60 sec		Truseq-HT-D5xx_F (10uM)	2.5	72℃	60 sec	
1391r primer 10uM (final 0.2uM	0.5	72℃	5 min	1 cycle	1391r primer 10uM (final 0.2uf	0.5	72℃	5 min	1 cycle	Truseq-HT-D7xx_R (10uM)	2.5	72℃	5 min	1 cycle
H2O	5	4℃	∞	1 cycle	895f_blocking_mito 20uM	2.5	4℃	∞	1 cycle	Total	50	10℃	forever	1 cycle
					895f_blocking_chloro_20uM	2.5								
Total	25				Total	25				25uL/tube				
Beads purificatin, 1:1					Beads purificatin, 1:1					Beads purificatin, 1:1				

Table S6. Metadata of harvested crown galls

#SampleID	Strain*	Year of inoculation	Month od inoculation	Day of inoculation	Year of harvest	Month of harvest	Day of harvest	Weight (g)
1115-11L	Δ*tssL*	2018	11	15	2019	1	18	1.80
1115-12L[a]	Δ*tssL*	2018	11	15	2019	1	18	0.81
1115-13L[a]	Δ*tssL*	2018	11	15	2019	1	18	0.62
1115-14L[a]	Δ*tssL*	2018	11	15	2019	1	18	0.96
1115-15L	Δ*tssL*	2018	11	15	2019	1	18	0.40
1115-16L	Δ*tssL*	2018	11	15	2019	1	18	0.40
1115-17L	Δ*tssL*	2018	11	15	2019	1	18	0.07
1115-18L	Δ*tssL*	2018	11	15	2019	1	18	0.16
1115-19W	WT	2018	11	15	2019	1	18	2.00
1115-20W	WT	2018	11	15	2019	1	18	1.27
1115-21W[b]	WT	2018	11	15	2019	1	18	0.56
1115-22W[b]	WT	2018	11	15	2019	1	18	0.56
1115-23W	WT	2018	11	15	2019	1	18	0.42
1115-24W	WT	2018	11	15	2019	1	18	0.37
1115-25W[b]	WT	2018	11	15	2019	1	18	0.82
1115-26W	WT	2018	11	15	2019	1	18	0.22
1115-27W	WT	2018	11	15	2019	1	18	0.10
1115-28W	WT	2018	11	15	2019	1	18	0.08
1115-29W	WT	2018	11	15	2019	1	18	0.05
1115-30W	WT	2018	11	15	2019	1	18	0.02
0704-1W	WT	2019	7	4	2019	9	2	0.12
0704-2W	WT	2019	7	4	2019	9	2	0.12
0704-3W	WT	2019	7	4	2019	9	2	0.09
0704-4W	WT	2019	7	4	2019	9	2	0.06
0704-5W	WT	2019	7	4	2019	9	2	0.11
0704-6W	WT	2019	7	4	2019	9	2	0.14
0704-7W	WT	2019	7	4	2019	9	2	0.27
0704-1L	Δ*tssL*	2019	7	4	2019	9	2	0.10
0704-2L	Δ*tssL*	2019	7	4	2019	9	2	0.34
0704-3L	Δ*tssL*	2019	7	4	2019	9	2	0.12
0704-4L	Δ*tssL*	2019	7	4	2019	9	2	0.07
0704-5L	Δ*tssL*	2019	7	4	2019	9	2	0.06
0704-6L	Δ*tssL*	2019	7	4	2019	9	2	0.10
0704-7L	Δ*tssL*	2019	7	4	2019	9	2	0.13

#SampleID	Strain*	Year of inoculation	Month od inoculation	Day of inoculation	Year of harvest	Month of harvest	Day of harvest	Weight (g)
0704-1B	Δ*tssB*	2019	7	4	2019	9	2	0.11
0704-2B	Δ*tssB*	2019	7	4	2019	9	2	0.28
0704-3B	Δ*tssB*	2019	7	4	2019	9	2	0.07
0704-4B	Δ*tssB*	2019	7	4	2019	9	2	0.22
0704-5B	Δ*tssB*	2019	7	4	2019	9	2	0.06
0722-1W	WT	2019	7	22	2019	9	28	0.03
0722-2W	WT	2019	7	22	2019	9	28	0.04
0722-3W	WT	2019	7	22	2019	9	28	0.07
0722-4W	WT	2019	7	22	2019	9	28	0.05
0722-5W	WT	2019	7	22	2019	9	28	0.13
0722-6W	WT	2019	7	22	2019	9	28	0.05
0722-1B	Δ*tssB*	2019	7	22	2019	9	28	0.01
0722-2B	Δ*tssB*	2019	7	22	2019	9	28	0.01
0729-1W	WT	2019	7	29	2019	9	29	0.03
0729-2W	WT	2019	7	29	2019	9	29	0.05
0729-3W	WT	2019	7	29	2019	9	29	0.04
0729-4W	WT	2019	7	29	2019	9	29	0.05
0729-5W	WT	2019	7	29	2019	9	29	0.04
0729-6W	WT	2019	7	29	2019	9	29	0.01
0729-7W	WT	2019	7	29	2019	9	29	0.05
0729-8W	WT	2019	7	29	2019	9	29	0.08
0729-9W	WT	2019	7	29	2019	9	29	0.03
0729-1L	Δ*tssL*	2019	7	29	2019	9	29	0.01
0729-2L	Δ*tssL*	2019	7	29	2019	9	29	0.05
0729-3L	Δ*tssL*	2019	7	29	2019	9	29	0.08
0729-4L	Δ*tssL*	2019	7	29	2019	9	29	0.03
0729-1B	ΔtssB	2019	7	29	2019	9	29	0.09
0729-2B	ΔtssB	2019	7	29	2019	9	29	0.07
1005-1W	WT	2019	10	5	2019	12	13	0.27
1005-2W	WT	2019	10	5	2019	12	13	0.16
1005-3W	WT	2019	10	5	2019	12	13	0.09
1005-4W	WT	2019	10	5	2019	12	13	0.04
1005-5W	WT	2019	10	5	2019	12	13	0.01
1005-6W	WT	2019	10	5	2019	12	13	0.09
1005-7W	WT	2019	10	5	2019	12	13	0.01

#SampleID	Strain*	Year of inoculation	Month od inoculation	Day of inoculation	Year of harvest	Month of harvest	Day of harvest	Weight (g)
1005-1L	Δ*tssL*	2019	10	5	2019	12	13	0.23
1005-2L	Δ*tssL*	2019	10	5	2019	12	13	0.32
1005-3L	Δ*tssL*	2019	10	5	2019	12	13	0.09
1005-4L	Δ*tssL*	2019	10	5	2019	12	13	0.04
1005-5L	Δ*tssL*	2019	10	5	2019	12	13	0.01
1005-1B	Δ*tssB*	2019	10	5	2019	12	13	0.23
1005-2B	Δ*tssB*	2019	10	5	2019	12	13	0.56
1005-3B	Δ*tssB*	2019	10	5	2019	12	13	0.16
1005-4B	Δ*tssB*	2019	10	5	2019	12	13	0.05
1005-5B	Δ*tssB*	2019	10	5	2019	12	13	0.06
1005-6B	Δ*tssB*	2019	10	5	2019	12	13	0.03
1005-7B	Δ*tssB*	2019	10	5	2019	12	13	0.06
1030-1W	WT	2019	10	30	2020	1	9	0.34
1030-2W	WT	2019	10	30	2020	1	9	0.12
1030-3W	WT	2019	10	30	2020	1	9	0.05
1030-4W	WT	2019	10	30	2020	1	9	0.03
1030-5W	WT	2019	10	30	2020	1	9	0.05
1030-6W	WT	2019	10	30	2020	1	9	0.11
1030-7W	WT	2019	10	30	2020	1	9	0.02
1030-8W	WT	2019	10	30	2020	1	9	0.01
1030-1L	Δ*tssL*	2019	10	30	2020	1	9	0.50
1030-2L	Δ*tssL*	2019	10	30	2020	1	9	0.07
1030-3L	Δ*tssL*	2019	10	30	2020	1	9	0.03
1030-4L	Δ*tssL*	2019	10	30	2020	1	9	0.01
1030-1B	Δ*tssB*	2019	10	30	2020	1	9	0.17
1030-2B	Δ*tssB*	2019	10	30	2020	1	9	0.06
1030-3B	Δ*tssB*	2019	10	30	2020	1	9	0.08
1030-4B	Δ*tssB*	2019	10	30	2020	1	9	0.00
1030-5B	Δ*tssB*	2019	10	30	2020	1	9	0.02
1030-6B	Δ*tssB*	2019	10	30	2020	1	9	0.01
1111-1W	WT	2019	11	11	2020	1	14	0.26
1111-2W	WT	2019	11	11	2020	1	14	0.19
1111-2.1W	WT	2019	11	11	2020	1	14	0.04
1111-3W	WT	2019	11	11	2020	1	14	0.25
1111-3.1W	WT	2019	11	11	2020	1	14	0.04

#SampleID	Strain*	Year of inoculation	Month od inoculation	Day of inoculation	Year of harvest	Month of harvest	Day of harvest	Weight (g)
1111-4W	WT	2019	11	11	2020	1	14	0.13
1111-5W	WT	2019	11	11	2020	1	14	0.01
1111-6W	WT	2019	11	11	2020	1	14	0.04
1111-7W	WT	2019	11	11	2020	1	14	0.05
1111-8W	WT	2019	11	11	2020	1	14	0.11
1111-8.1W	WT	2019	11	11	2020	1	14	0.09
1111-8.2W	WT	2019	11	11	2020	1	14	0.09
1111-9W	WT	2019	11	11	2020	1	14	0.02
1111-10W	WT	2019	11	11	2020	1	14	0.07
1111-11W	WT	2019	11	11	2020	1	14	0.02
1111-12W	WT	2019	11	11	2020	1	14	0.04
1111-13W	WT	2019	11	11	2020	1	14	0.27
1111-13.1W	WT	2019	11	11	2020	1	14	0.18
1111-13.2W	WT	2019	11	11	2020	1	14	0.12
1111-14W	WT	2019	11	11	2020	1	14	0.04
1111-15W	WT	2019	11	11	2020	1	14	0.01
1111-1L	Δ*tssL*	2019	11	11	2020	1	14	0.21
1111-2L	Δ*tssL*	2019	11	11	2020	1	14	0.04
1111-2.1L	Δ*tssL*	2019	11	11	2020	1	14	0.02
1111-3L	Δ*tssL*	2019	11	11	2020	1	14	0.07
1111-3.1L	Δ*tssL*	2019	11	11	2020	1	14	0.03
1111-4L	Δ*tssL*	2019	11	11	2020	1	14	0.03
1111-5L	Δ*tssL*	2019	11	11	2020	1	14	0.08
1111-6L	Δ*tssL*	2019	11	11	2020	1	14	0.08
1111-7L	Δ*tssL*	2019	11	11	2020	1	14	0.14
1111-8L	Δ*tssL*	2019	11	11	2020	1	14	0.01
1111-9L	Δ*tssL*	2019	11	11	2020	1	14	0.03
1111-1B	Δ*tssB*	2019	11	11	2020	1	14	0.18
1111-2B	Δ*tssB*	2019	11	11	2020	1	14	0.09
1111-3B	Δ*tssB*	2019	11	11	2020	1	14	0.03
1111-4B	Δ*tssB*	2019	11	11	2020	1	14	0.03
1111-5B	Δ*tssB*	2019	11	11	2020	1	14	0.02
1111-6B	Δ*tssB*	2019	11	11	2020	1	14	0.03

#SampleID	Strain*	Year of inoculation	Month od inoculation	Day of inoculation	Year of harvest	Month of harvest	Day of harvest	Weight (g)
1111-7B	Δ*tssB*	2019	11	11	2020	1	14	0.01
1111-8B	Δ*tssB*	2019	11	11	2020	1	14	0.01

* *Agrobacterium tumefaciens* C58 wilt type.

[a] Used in round I sequencing.

[b] Used in both round I and II sequencing.

Table S7. Crown gall metadata used for analysis of amplicon sequencing round III

#SampleID	Strain	Year_of_inoculation	Month_of_inoculation	Weight	Seasons	Trials	Bactch
#q2:types	categorical	categorical	categorical	numeric	categorical	categorical	categorical
1115-L12	tssL	2018	Nov	0.81	Winter	181115	Batch 1
1115-L13	tssL	2018	Nov	0.62	Winter	181115	Batch 1
1115-L14	tssL	2018	Nov	0.96	Winter	181115	Batch 1
1115-W21	C58 WT	2018	Nov	0.56	Winter	181115	Batch 1
1115-W22	C58 WT	2018	Nov	0.56	Winter	181115	Batch 1
1115-W25	C58 WT	2018	Nov	0.82	Winter	181115	Batch 1
0704-W1	C58 WT	2019	Jul	0.12	Summer	190704	Batch 4
0704-W2	C58 WT	2019	Jul	0.12	Summer	190704	Batch 4
0704-W3	C58 WT	2019	Jul	0.09	Summer	190704	Batch 4
0704-W4	C58 WT	2019	Jul	0.06	Summer	190704	Batch 4
0704-W5	C58 WT	2019	Jul	0.11	Summer	190704	Batch 4
0704-W6	C58 WT	2019	Jul	0.14	Summer	190704	Batch 4
0704-W7	C58 WT	2019	Jul	0.27	Summer	190704	Batch 4
0704-L1	tssL	2019	Jul	0.1	Summer	190704	Batch 4
0704-L2	tssL	2019	Jul	0.34	Summer	190704	Batch 4
0704-L3	tssL	2019	Jul	0.12	Summer	190704	Batch 4
0704-B1	tssB	2019	Jul	0.11	Summer	190704	Batch 4
0704-B2	tssB	2019	Jul	0.28	Summer	190704	Batch 4
0704-B3	tssB	2019	Jul	0.07	Summer	190704	Batch 4
1005-W1	C58 WT	2019	Oct	0.27	Summer	191005	Batch 7
1005-W2	C58 WT	2019	Oct	0.16	Summer	191005	Batch 7
1005-W3	C58 WT	2019	Oct	0.09	Summer	191005	Batch 7
1005-W6	C58 WT	2019	Oct	0.09	Summer	191005	Batch 7
1005-L1	tssL	2019	Oct	0.23	Summer	191005	Batch 7
1005-L2	tssL	2019	Oct	0.32	Summer	191005	Batch 7
1005-L3	tssL	2019	Oct	0.09	Summer	191005	Batch 7
1005-B1	tssB	2019	Oct	0.23	Summer	191005	Batch 7
1005-B2	tssB	2019	Oct	0.56	Summer	191005	Batch 7
1005-B3	tssB	2019	Oct	0.16	Summer	191005	Batch 7
1005-B5	tssB	2019	Oct	0.06	Summer	191005	Batch 7
1005-B7	tssB	2019	Oct	0.06	Summer	191005	Batch 7
1030-W1	C58 WT	2019	Oct	0.34	Winter	191030	Batch 8
1030-W2	C58 WT	2019	Oct	0.12	Winter	191030	Batch 8
1030-W6	C58 WT	2019	Oct	0.11	Winter	191030	Batch 8
1030-L1	tssL	2019	Oct	0.5	Winter	191030	Batch 8

#SampleID	Strain	Year_of_inoculation	Month_of_inoculation	Weight	Seasons	Trials	Bactch
1030-L2	tssL	2019	Oct	0.07	Winter	191030	Batch 8
1030-B1	tssB	2019	Oct	0.17	Winter	191030	Batch 8
1030-B2	tssB	2019	Oct	0.06	Winter	191030	Batch 8
1030-B3	tssB	2019	Oct	0.08	Winter	191030	Batch 8
1111-W1	C58 WT	2019	Nov	0.26	Winter	191111	Batch 9
1111-W2	C58 WT	2019	Nov	0.19	Winter	191111	Batch 9
1111-W3	C58 WT	2019	Nov	0.25	Winter	191111	Batch 9
1111-W4	C58 WT	2019	Nov	0.13	Winter	191111	Batch 9
1111-W8	C58 WT	2019	Nov	0.11	Winter	191111	Batch 9
1111-W10	C58 WT	2019	Nov	0.07	Winter	191111	Batch 9
1111-W13	C58 WT	2019	Nov	0.27	Winter	191111	Batch 9
1111-L1	tssL	2019	Nov	0.21	Winter	191111	Batch 9
1111-L3	tssL	2019	Nov	0.07	Winter	191111	Batch 9
1111-L5	tssL	2019	Nov	0.08	Winter	191111	Batch 9
1111-L6	tssL	2019	Nov	0.08	Winter	191111	Batch 9
1111-L7	tssL	2019	Nov	0.14	Winter	191111	Batch 9
1111-B1	tssB	2019	Nov	0.18	Winter	191111	Batch 9
1111-B2	tssB	2019	Nov	0.09	Winter	191111	Batch 9

References

1. Wood, D.W., et al., The genome of the natural genetic engineer *Agrobacterium tumefaciens* C58. Science, 2001. **294**(5550): p. 2317-23.
2. Lin, J.S., L.S. Ma, and E.M. Lai, Systematic Dissection of the *Agrobacterium* Type VI Secretion System Reveals Machinery and Secreted Components for Subcomplex Formation. PLoS One, 2013. **8**(7): p. e67647.
3. Liu, A.C., et al., A citrate-inducible gene, encoding a putative tricarboxylate transporter, is downregulated by the organic solvent DMSO in *Agrobacterium tumefaciens*. J Appl Microbiol, 2008. **105**(5): p. 1372-1383.